J. Earth Syst. Sci. (2018) 127:16
https://doi.org/10.1007/s12040-018-0917-4

Probabilistic seismic hazard at the archaeological site of Gol Gumbaz in Vijayapura, south India

Shivakumar G Patil, Arun Menon* and G R Dodagoudar

Department of Civil Engineering, Indian Institute of Technology Madras, Chennai 600 036, India.
**Corresponding author. e-mail: arunmenon@iitm.ac.in*

MS received 14 February 2017; revised 15 June 2017; accepted 8 July 2017; published online 2 March 2018

Probabilistic seismic hazard analysis (PSHA) is carried out for the archaeological site of Vijayapura in south India in order to obtain hazard consistent seismic input ground-motions for seismic risk assessment and design of seismic protection measures for monuments, where warranted. For this purpose the standard Cornell-McGuire approach, based on seismogenic zones with uniformly distributed seismicity is employed. The main features of this study are the usage of an updated and unified seismic catalogue based on moment magnitude, new seismogenic source models and recent ground motion prediction equations (GMPEs) in logic tree framework. Seismic hazard at the site is evaluated for level and rock site condition with 10% and 2% probabilities of exceedance in 50 years, and the corresponding peak ground accelerations (PGAs) are 0.074 and 0.142 g, respectively. In addition, the uniform hazard spectra (UHS) of the site are compared to the Indian code-defined spectrum. Comparisons are also made with results from National Disaster Management Authority (NDMA 2010), in terms of PGA and pseudo spectral accelerations (PSAs) at $T = 0.2$, 0.5, 1.0 and 1.25 s for 475- and 2475-yr return periods. Results of the present study are in good agreement with the PGA calculated from isoseismal map of the Killari earthquake, $M_w = 6.4$ (1993). Disaggregation of PSHA results for the PGA and spectral acceleration (S_a) at 0.5 s, displays the controlling scenario earthquake for the study region as low to moderate magnitude with the source being at a short distance from the study site. Deterministic seismic hazard (DSHA) is also carried out by taking into account three scenario earthquakes. The UHS corresponding to 475-yr return period (RP) is used to define the target spectrum and accordingly, the spectrum-compatible natural accelerograms are selected from the suite of recorded accelerograms.

Keywords. Seismic hazard; GMPEs; PGA; uniform hazard spectra; spectrum-compatible natural accelerograms.

1. Introduction

Just as many other natural hazards, earthquakes pose major economic and societal consequences as can be seen over time and again in the aftermath of the many large earthquakes worldwide. The Indian subcontinent witnessed some of the greatest earthquakes in the world. According to Building Materials and Technology Promotion Council (BMTPC) of Government of India, 59% of the total land mass of the country is prone to earthquakes (BMTPC 1997). Peninsular India (PI) is no exception as far as the seismic hazard is concerned. In order to assess the risk to a structure or facility from the ground shaking hazard induced by earthquakes, we must first estimate the ground-motion

intensities from an earthquake at a particular site and evaluate the structure of interest under that intensity for its seismic performance. The quantitative assessment of ground-motion intensities in PI is challenging, although damaging earthquakes of severe to moderate magnitudes have occurred (e.g., Kutch 1819 M_w 7.8; Koyna 1967 M_w 6.3; Killari–Latur 1993 M_w 6.4; Jabalpur 1997 M_w 5.7 and Bhuj 2001 M_w 7.7), but the general level of seismicity is subdued. Probabilistic seismic hazard studies for the region are limited even after the devastating 1993 Killari M_w 6.4 earthquake, in which 7928 persons were killed (Jain 2016). A few studies (NDMA 2010; Nath and Thingbaijam 2012) were carried out for the entire land mass of the India, however they have adopted rather coarse grid size and seismic zonation for the region; hence the results may be indicative. Some of the previous researchers (Jaiswal and Sinha 2007; Sitharam *et al.* 2012; Desai and Choudhury 2013) used global GMPEs which are based on limited data compared to recent Next Generation Attenuation (NGA) models. Selection and ranking of the appropriate GMPEs for modelling the intrinsic epistemic uncertainty can be challenging, given the fact that their number has significantly increased (Douglas 2016). Some studies have been attempted in assigning a ranking system for selection of the GMPEs based on data driven methods (Nath and Thingbaijam 2011; Anbazhagan *et al.* 2013, 2016). In the present study, the appropriate ranking system has been used for the selection of GMPEs based on the trellis plots. The use of the most recent GMPEs (Next Generation Attenuation Models, NGA-W2, NGA-East, pan-European models) is anticipated to minimise the uncertainty incurred due to arbitrary selection and use of older models.

Heritage structures are precious as they form inextricable components of history, culture and human evolution. They are testimony to the ancient building technology, aesthetics, cultural practices, arts, defences and governance of the region. These buildings are the main source of revenue for local governments and community, and in many countries such as India, form part of the living heritage. Historical masonry structures were built based on empirical knowledge of structural behaviour, such a trial-and-error process mainly took care of static loads, but they are often vulnerable to dynamic loads such as earthquakes because of a large mass of its masonry walls, poor connections between structural elements and structural distress due to deteriorated material properties. Conservation of such historical buildings from natural disasters is the paramount responsibility of the modern society so that it may be preserved for future generations. National Policy for Conservation of the Ancient Monuments, Archaeological Sites and Remains (NPC-AMASR 2014) protected by the Archaeological Survey of India (ASI) requires monuments and their structural components such as material and construction technique to be evaluated to ascertain their behaviour, and to undertake necessary minimum retrofitting measures of the monument. This would mitigate possible damages to structures and facilities during and after disasters. In this regard, seismic safety assessment of historical built heritage requires seismic inputs in the form of hazard curves, uniform hazard spectra and spectrum-compatible natural acceleration time-histories.

In this study, probabilistic seismic hazard analysis (PSHA) is carried out to estimate the seismic hazard due to ground-motion at the archaeological site of Gol Gumbaz, Vijayapura, which lies in the state of Karnataka, and is about 384 km west of the city of Hyderabad in south India (see figure 1a). Vijayapura city is a testimony to Indo-Islamic architecture built during the rule of the Adil Shahi Dynasty. The Gol Gumbaz, a monumental structure, which is the mausoleum of Muhammad Adil Shah (AD 1626–1656), is world famous among several other monuments of Indo-Islamic architecture (see figure 1b). The Gol Gumbaz is known for its sheer massiveness, unique acoustic feature and it is roofed with a masonry dome that came to be rated as the fourth largest in the world (Scandella *et al.* 2011), and first in terms of uninterrupted area covered (1672 m^2). Seismic history of the city dates back to 1653–1654 AD; there is a mention about the occurrence of an earthquake in the book 'Basatin-us-Salatin', a history of Vijayapura from origin of the dynasty to its last representative records by Muhammad Ibrahim Zuberi (Iyenger *et al.* 1999a). The largest recorded earthquakes in the region around Gol Gumbaz, Vijayapura are M_w 6.4 Killari earthquake, 1993 (160 km from the site) and M_w 6.3 Koyna earthquake, 1967 (226 km from the site) (refer figure 1a). There are no strong-motion records available for these earthquakes. The isoseismal map of the M_w 6.4 Killari earthquake (refer figure 2) shows that during the event the area had experienced an intensity of VI on the Modified Mercalli Intensity scale (MMI).

Seismic input plays a very important role in seismic risk estimation and design of seismic

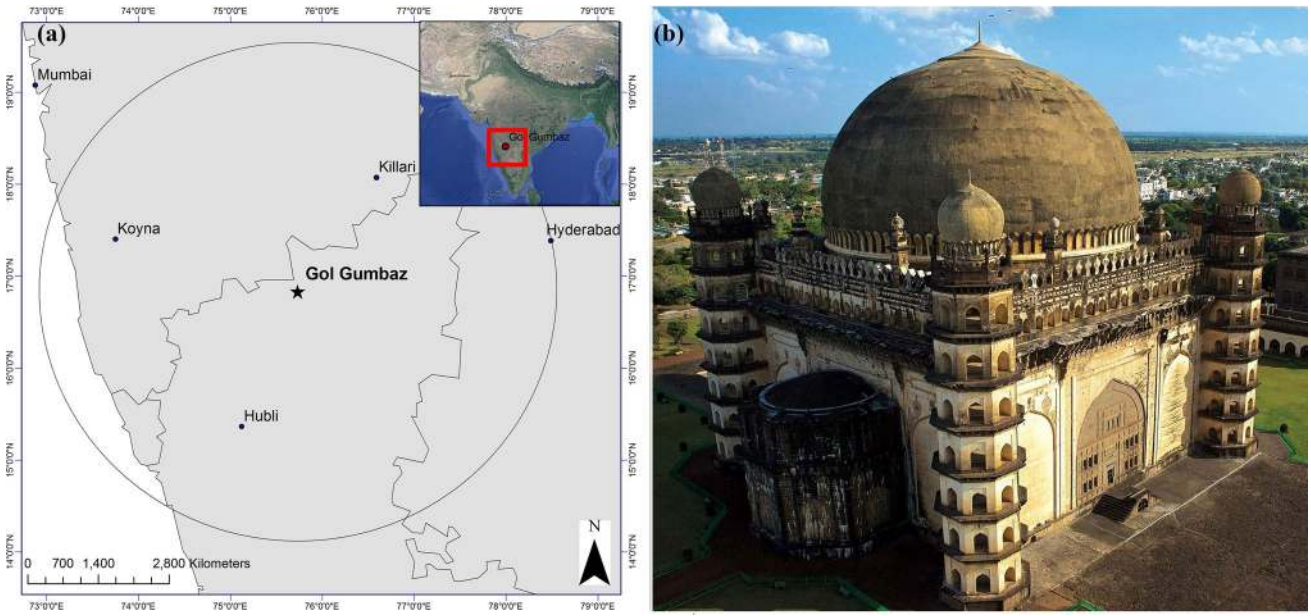

Figure 1. **(a)** Inset: Map of India showing the area of study (open square). Map of PI showing the location of the archaeological site, Gol Gumbaz, large circle indicates the control region. **(b)** Gol Gumbaz.

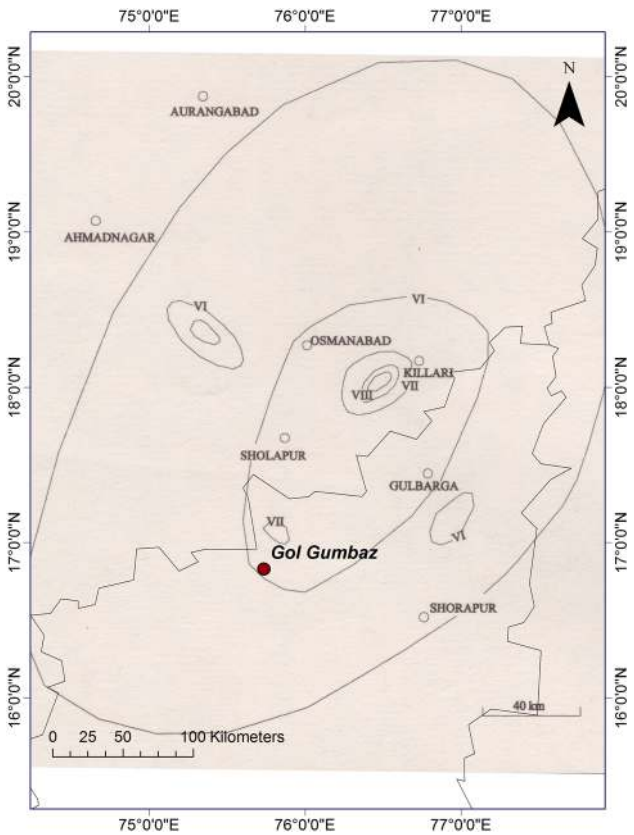

Figure 2. Isoseismal map of 1993 Killari earthquake (modified after GSI 2000).

retrofitting measures for historical monuments. PSHA is a widely used tool to quantitatively assess the nature of earthquake ground-motions at a particular site due to future earthquakes occurring in and around the site, within an influence region, in a specified time frame. This paper describes the state-of-the-art PSHA methodology aimed at producing the probabilistic hazard curve, uniform hazard spectrum (UHS) for reference return periods (i.e., 72, 224, 475, 975 and 2,475 yrs) and spectrum compatible accelerograms on stiff and level ground at the archaeological site of Gol Gumbaz. The standard Cornell–McGuire approach has been used for the PSHA, which was first formalized in late 1960s by Cornell (1968) and generalized by McGuire (1976). The study has utilized a unified seismic catalogue based on moment magnitude, new seismogenic sources and recent ground-motion prediction equations (GMPEs) within the logic tree framework to evaluate the hazard at the site.

2. Tectonic setting and geology

India separated from supercontinent Gondwanaland about 140 million years ago, and it was moving with high speed (i.e., 18–20 cm/yr), which gradually slowed to ≈ 5 cm/yr after continental collision with Asia about 50 million years ago (Kumar *et al.* 2007). The south India plate is a combination of several crustal blocks formed by geodynamic processes operating from mid-Archaean to Neo-Proterozoic time (Gupta *et al.* 2003). For a very long geological period, these crustal blocks have not undergone deformation. PI consists of four major cratonic features: Dharwar, Bastar,

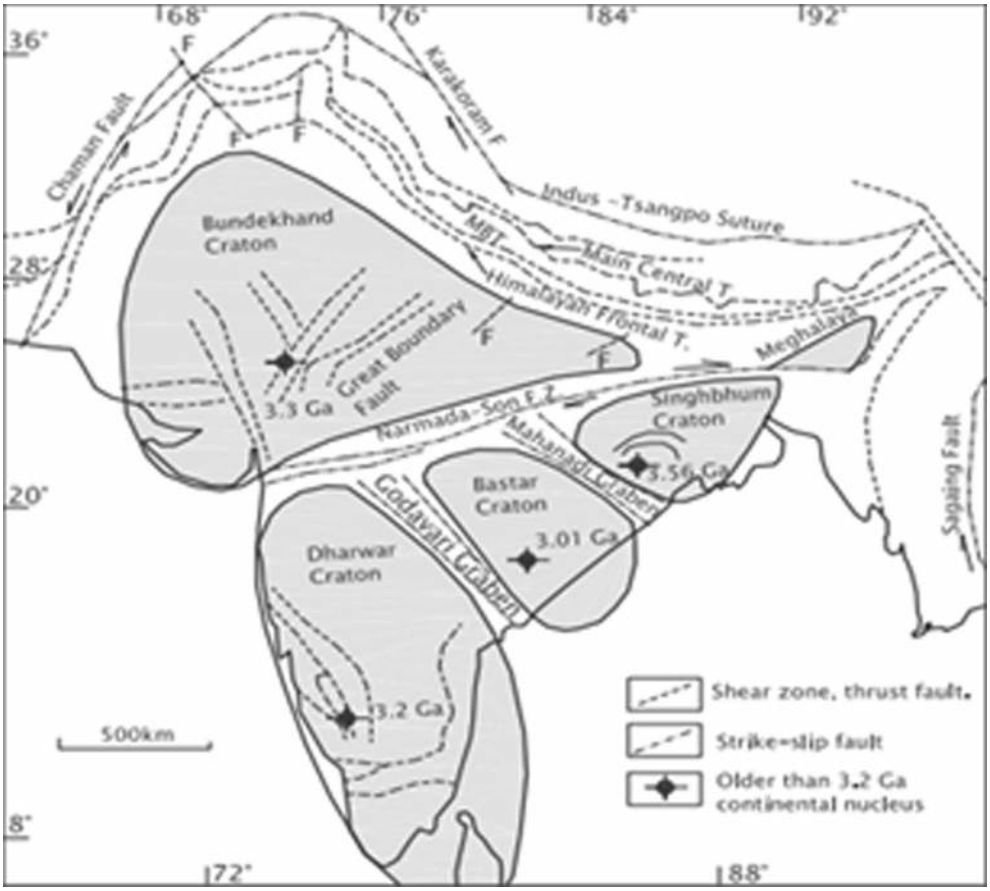

Figure 3. Cratonic blocks of PI made up of various rock complexes of Archean Eon (Valdiya 2016).

Singhbhum and Bundelkhand Cratons in southern, central, eastern and western India, respectively (Valdiya 2016). The major prominent rifts are (i) Son–Narmada rift valley which demarcates the northern and southern Cratons, (ii) Mahanadi graben which separates the Singhbhum Craton from the Bastar Craton, and (iii) Godavari rift valley which separates the Bastar and the Dharwar Cratons (Valdiya 2016) (refer figure 3).

Earthquakes in India are characterized by relatively frequent large earthquake and relatively infrequent moderate earthquakes (M > 6 to 7), making earthquake risk mitigation a challenge. About 0.5% of global strain energy is released in the form of intraplate earthquakes along the weak zones present in the plate interior (Johnston and Kanter 1990; Mandal *et al.* 1997). These intraplate earthquakes are mainly attributed to strain energy release by sudden movement a long pre-existing weak zones in response to stress disruption, which is caused by forces along plate boundary or by localized weakening of crustal materials, surface and subsurface loading and reservoir loading (Mandal *et al.* 1997). The PI produced both rift and non-rift associated earthquakes (refer figure 4).

Copley *et al.* (2014) suggested two main causes for the seismicity in PI. The first one proposed by Bilham *et al.* (2003) noted that the Indian plate underthrusts the Tibetan Plateau causing flexural bulge in central India and flexural trough in the southern India. The observed distribution of earthquakes and seismic energy release are consistent with these bulge and trough bending stresses. The recent Killari (1993) and Bhuj (2001) earthquakes occurred near to this region of high-stress concentration. Similarly, Vita-Finzi (2004) reviewed large earthquakes (M > 5) of PI and concluded that majority of them occurred on reverse faults indicating shortening of azimuth between NW–SE and NE–SW or on strike-slip faults oriented NNE. Based on these studies, Vita-Finzi proposed the spatial distribution of large earthquakes in PI, based on buckling resulting from plate convergence. In lieu, Copley *et al.* (2014) proposed that "the fluid pressure that is exerted on the Indian peninsula due to the difference in crustal thickness between India and the Tibetan Plateau

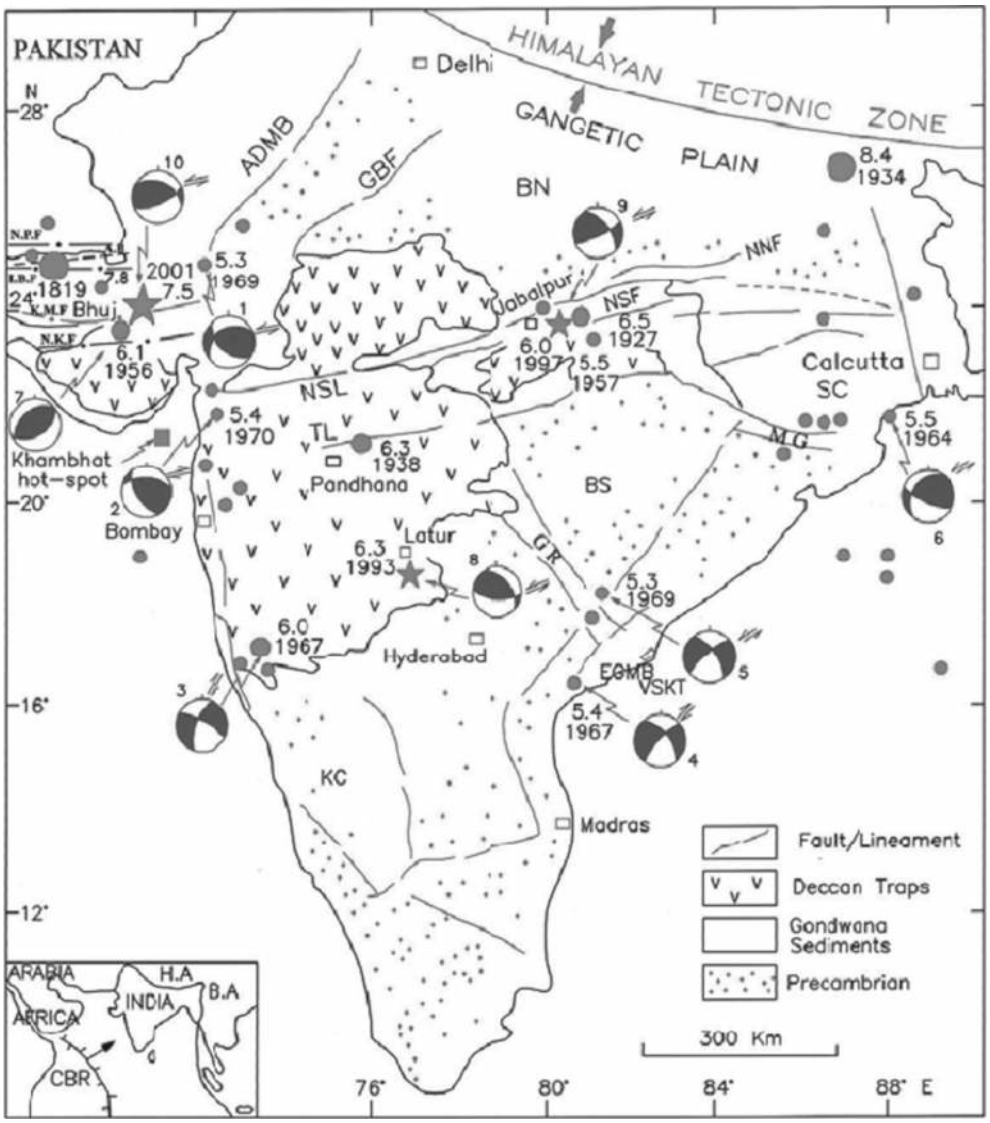

Figure 4. Seismotectonic units of PI with prominent earthquakes with fault plane solution and major faults, lineaments and rifts (Kayal 2000).

is enough to reactivate the faults". Both these mechanisms would result in dip-slip faulting as observed in PI (1993 Killari, 1997 Jabalpur and 2003 Bhuj earthquakes). Most parts of the PI are characterized by diffused seismicity; nevertheless, several localized seismicity associated with rift and shear/thrust zones can be observed. Vijayapura situated in the geological provinces of Dharwar Craton is an Archaean continental fragment of the PI.

2.1 *Trends in regional seismicity and potential seismic sources*

PI resides within an intraplate setting (a region far from well-defined plate boundaries) in which very little crustal deformation is observed. Hence earthquakes are generally less likely to occur than near plate boundaries, as in the foothills of the mighty Himalayas. There are 30 neotectonic faults in stable PI, mostly limited to paleorift systems (Verma and Bansal 2016). It is to be noted that the information on the fault-plane geometry, mechanism (strike-slip, normal, oblique, thrust or subduction), extension, and activity rates is inadequate in order to adopt these faults within a PSHA framework. Paleoseismological studies constrained the recurrence intervals of the earthquake in the stable continental regions such as PI to 10,000 years (Verma and Bansal 2016).

The control region considered for the present study includes a circular area of 300 km radius considering Gol Gumbaz, Vijayapura as its centre.

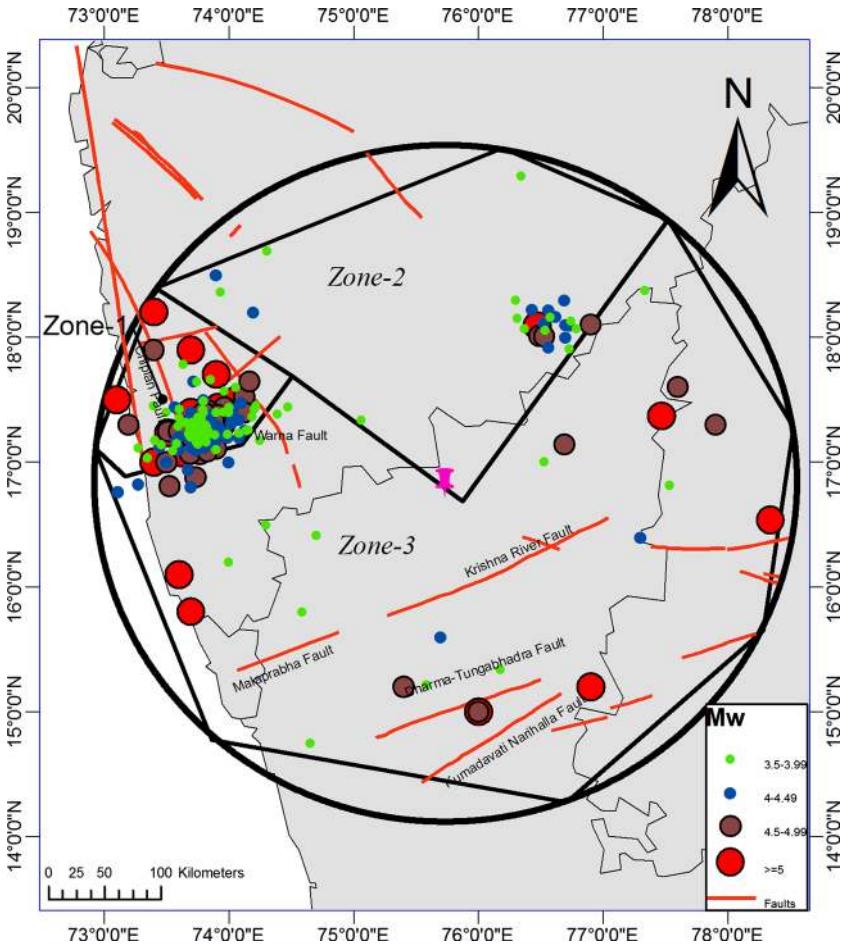

Figure 5. Seismogenic zonation composed of three zones along with digitized faults and epicenters of earthquakes.

In this control region, many faults, lineaments, shear zones have been identified, and different seismic events compiled. The Geological Survey of India (GSI 2000) prepared and published an atlas entitled Seismotectonic Atlas of India and its Environs, which contains 43 maps in 42 sheets covering India and adjoining regions of neighbouring countries on 1:1 million scale (Dasgupta *et al.* 2000). This has been taken as a reliable reference for digitizing and georeferencing various earthquake sources such as faults, lineaments and shear zones using ArcMap in separate layers. Various researchers such as Anbazhagan *et al.* (2009) for Bangalore, Desai and Choudhury (2013) for Mumbai, James *et al.* (2014) for Kalpakkam nuclear power plant site and Anbazhagan *et al.* (2017) for Kanpur have used these maps for seismic source characterization. The earthquake catalogue is superimposed on this digitized tectonic source map and all layers are combined to form the complete source map (figure 5). The ENE–WSW trending Krishna River fault runs halfway along the Krishna River and Dharma–Tungabhadra fault runs all along the Tungabhadra River in ENE–WSW direction. These two faults are treated as fault sources in proximity to the archaeological site at Vijayapur. Within the study area, background seismicity is concentrated in the Koyana–Warna and Killari regions. Majority of the earthquakes in these regions cannot be attributed to particular faults. There are 23 earthquakes of $M_w \geq 5.0$, about 215 earthquakes of M_w 4.0−5.0, and many smaller earthquakes. There are considerable debates about the causes of earthquakes (induced *vs.* tectonic) in these areas. Diffuse bands of seismicity are present in the southern region of the study area (see figure 5).

3. Earthquake catalogue

Collection of well-defined earthquake catalogue is an important step in order to model seismic sources along with thorough understanding of

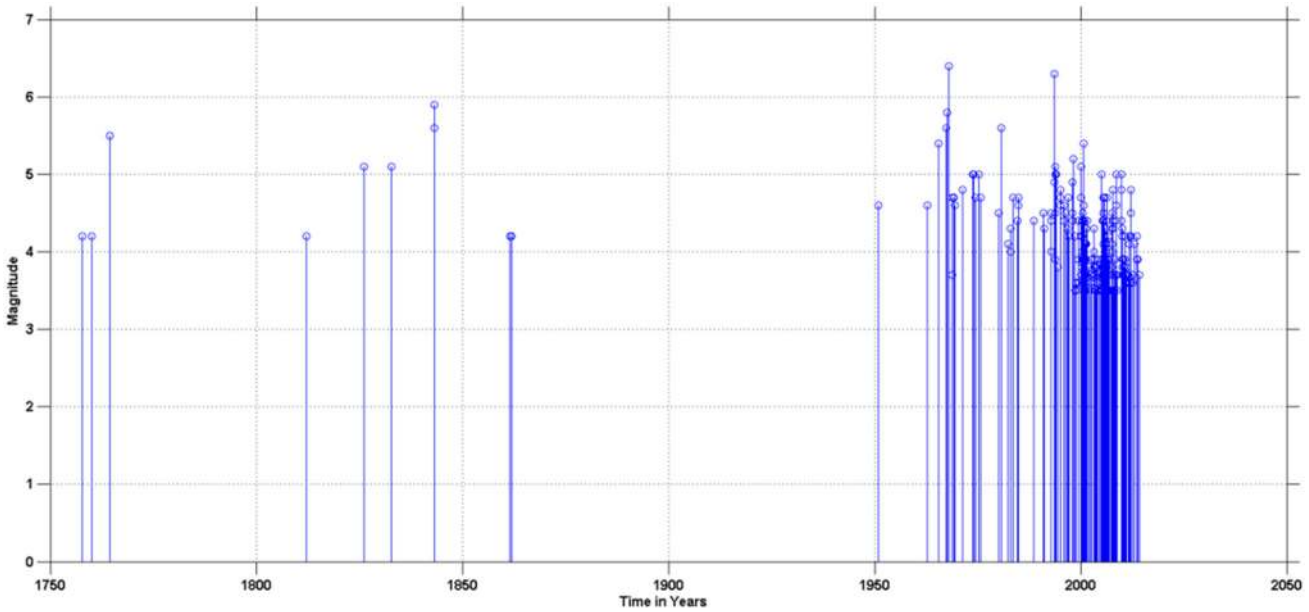

Figure 6. Temporal distribution of earthquakes in the study area.

seismotectonic, geological settings of the study area. Thus, preparation of an updated, composite and homogeneous, earthquake catalogue is the starting point in any PSHA study. An updated composite earthquake catalogue for Vijayapura within a control area of 300 km radius (the choice of radius being dictated by the distances to the seismic source zones that contribute to seismic hazard at the site) has been compiled from different internationally recognized earthquake database agencies such as, India Meteorological Department (IMD), National Earthquake Information Center (NEIC), International Seismological Center (ISC) and Global Centroid-Moment Tensors (GCMT). Historical and instrumented earthquakes have also been compiled from the published literature (Chandra 1977; Rao and Rao 1984; Guha and Basu 1993; Iyenger *et al.* 1999; Jaiswal and Sinha 2007). When earthquake data is collected from different agencies, there is always the possibility of reporting the same event more than once. Such duplicate events are removed by comparing the location, time of occurrence and magnitude of each event. It is necessary to homogenize the measure of earthquake magnitude in a composite catalogue into moment magnitude M_w, because of its clear relationship with the physical property of the source (seismic moment). Johnston (1996) proposed empirical equations based on worldwide data of events from stable continental regions (SCR), including India, to convert the body-wave magnitude (m_b), local magnitude (M_L) and surface wave magnitude (M_s) to the moment magnitude (M_w). The pre-instrumental earthquakes, expressed qualitatively in terms of macroseismic epicentral intensity (I_0), are converted into M_w using an empirical conversion relationship proposed by Menon *et al.* (2010) for peninsular Indian earthquakes. The composite catalogue for Vijayapura spans 257 years from 1757 to April 2016 AD consisting of 437 earthquakes with $M_w \geq 3$ (refer figure 6).

4. Processing of earthquake catalogue

4.1 *Declustering*

Declustering is the process of separation of the clusters involving foreshocks and aftershocks from the main earthquake events. The computational approach to PSHA is based on the widely used Poisson model, which assumes that earthquake occurrences are spatially and temporally independent events. In order to fulfill the assumption of a Poisson process, it is necessary to identify the earthquake clusters (dependent events) and remove them from the earthquake catalogue. The declustering algorithm developed by Gardner and Knopoff (1974) for southern California, implemented in ZMAP software (Wiemer 2001), has been used in the study. This algorithm assumes magnitude dependent spatial and temporal window for removal of foreshocks and aftershocks. Figure 7(a) shows the spatial distribution of declustered catalogue containing 224 main events,

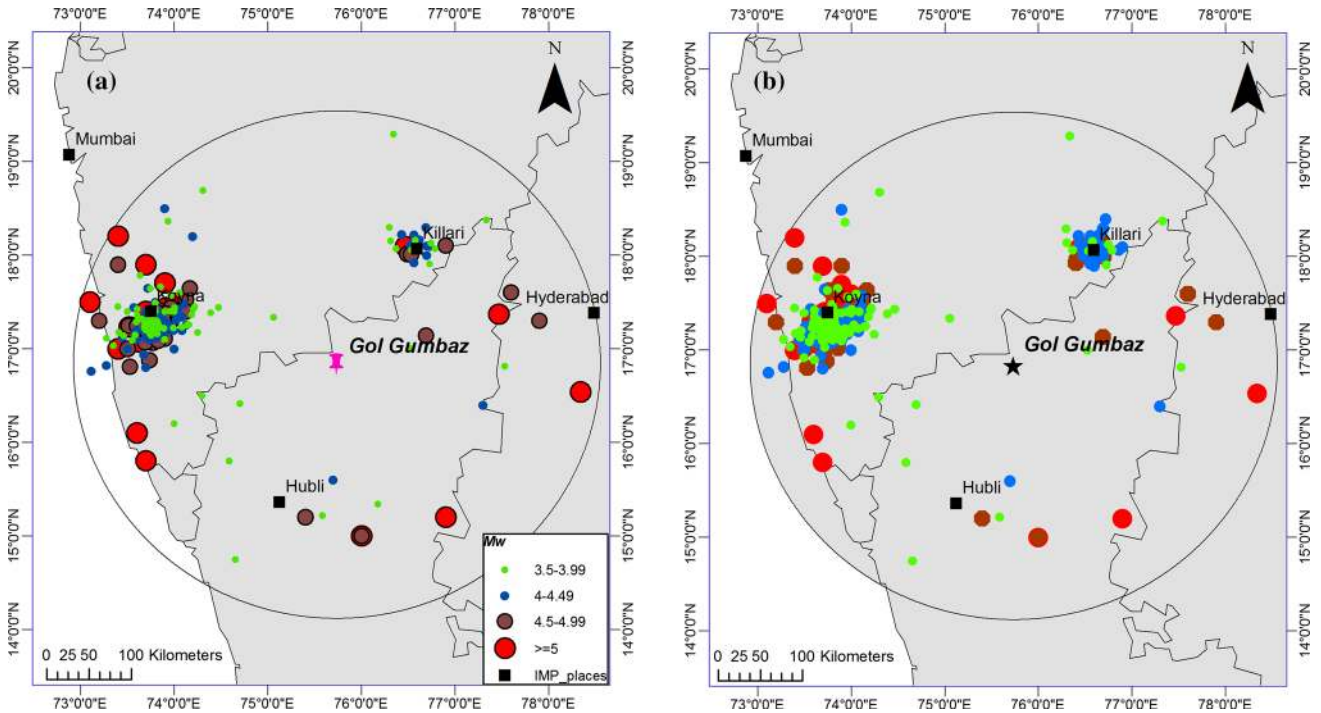

Figure 7. Maps showing the spatial distribution of seismicity of the region from 1757 AD: **(a)** after declustering and **(b)** before declustering.

whereas figure 7(b) shows all the events including the main events. There were about 96 clusters, which constitute 200 dependent events out of a total of 424 events, i.e., 47.2% of the events have been removed.

4.2 *Estimation of completeness periods*

Completeness levels of the catalogue must be checked before using them for earthquake rate calculation. The completeness period defines the magnitude above which all earthquakes have been included in that period. Thus, the completeness level depends on time and reflects historical patterns of the colony (i.e., settlements of human beings to report an occurrence of the earthquake) and availability of seismic instrumentation. Small earthquakes in historical records may go unnoticed depending on the demography of the region. Hence, historical catalogues are generally more complete for larger magnitudes. There are many methods to check the completeness of the catalogue. In the present study statistical approaches are used, which is based on the cumulative number of events against time. In the assumption of Poisson distribution, the plot between the cumulative rates of events vs. time should remain constant; hence, variations in this rate can be seen as incompleteness. In these approaches, the periods of completeness for different magnitude intervals are inferred by identifying breaks in the slope on a linear plot of cumulative rate against time. Completeness analysis has been performed for different magnitude bins having bin width = 0.5, and for each of the seismogenic zones. Two different methods are chosen to perform the completeness analysis, viz., CUVI (Visual Cumulative) method (Tinti and Mulargia 1985) and Stepp method adopting a bin width = 0.5 and 10-yr time intervals (Stepp 1972). The completeness periods for different magnitude ranges are summarized in table 1.

5. Methodology

Seismic hazard analysis of any given site consists of two main models: firstly, the seismic source characterization (SSC) model, which quantitatively describes all possible earthquake sources with the help of seismotectonic and geological data along with the earthquake catalogue in the vicinity of the site (generally about 300 km radius from the site of interest) and, secondly a ground-motion (GM) model, expressed by the ground-motion prediction equation (GMPE), which estimates the expected distribution of ground-motion parameters (e.g., spectral acceleration) at a site due to a particular

Table 1. *The G–R recurrence parameters and completeness periods for different magnitude bins.*

Scenario	Zone	M_w range	Method	b	a	$M_w \geq 3.5$	$M_w \geq 4$	$M_w \geq 4.5$	$M_w \geq 5$	$M_w \geq 5.5$
I	X	3.5–6.4	Visual	1.09	5.13	1998	1982	1968	1965	1764
			Stepp	1.09	4.96	1984	1984	1964	1824	1774
II	1	3.5–6.4	Visual	1.16	5.43	1998	1997	1991	1993	1764
			Stepp	1.04	4.63	1975	1975	1965	1965	1745
	2	3.5–6.3	Visual	0.83	3.27	2000	1992	1993	–	–
			Stepp	0.76	2.87	1995	1985	1993	–	–
	3	3.5–5.9	Visual	1	4.0	1998	1997	1993	1826	–
			Stepp	0.83	3.07	1995	1975	1965	1815	–

earthquake scenario. The GMPE is characterized by a logarithmic mean value and an associated logarithmic standard deviation also called sigma which represents intrinsic variability.

5.1 *Seismic source characterization*

Seismic source characterization is a suite of locations, geometries, magnitudes and recurrence rates of seismic sources affecting the concerned site (Senior Seismic Hazard Analysis Committee, SSHAC 1997). There are always uncertainties in these descriptors, hence one can include alternative models and model parameters in a logic tree framework with appropriate weighting factors. The seismic sources are usually represented as line sources (i.e., faults) or area sources. In this study area seismic sources, also referred to as seismic zones have been employed. They are often used where specific fault data and long historic earthquake records do not exist (Molina *et al.* 2001; Allen *et al.* 2015), but large earthquakes might reasonably be expected based on seismotectonic analogues, such as in the PI. Area sources assume a uniform rate of earthquake occurred within the spatial region. Therefore, every location within the area has an equal probability that an event will occur. The hazard in some regions is sensitive to the placement of boundaries of a source zone. In this study, an effort has been made to delineate source boundaries based on the knowledge of seismotectonics, geological and historical seismicity (see figure 5). Furthermore, two seismic zone scenarios have been included in the present study.

In seismic zone scenario I (SZI), the entire circular area of the control region is considered as one source zone (see figure 7a). This criterion, by and large, conforms to the previous studies by Chandra (1977), Gupta (2006), National Disaster Management Authority (NDMA 2010) and Kolathayar and Sitharam (2012).

Seismic zone scenario II (SZII) is mainly based on the regional seismotectonic and seismicity of the study area. This scenario consists of three zones: Zone 1, Zone 2 and Zone 3 (see figure 5). Zone 1 covers the NW region, largely populated with earthquakes due to the Koyna–Warna reservoir region, which consists of the north-westerly trending Warna and Chiplun faults. Zone 2 covers parts of NW and NE regions consisting of the Latur lineament and the Upper Godavari faults. Zone 3 comprises the southern region with the Krishna river fault and the Bennihall lineament.

5.1.1 *Recurrence model*

The distribution of earthquake magnitude of identified seismic sources in a given period is described by Guttenberg–Richter (G–R) recurrence relationship (Gutenberg and Richter 1944). Based on the results of two completeness analysis methods, the parameters of the G–R recurrence relationship, 'a' and 'b' are determined (see table 1). Since the original G–R relationship suffers from boundlessness, a double-truncated G–R recurrence law (McGuire and Arabasz 1990; Kramer 1996) involving a lower threshold magnitude, $M_{min} = 3.5$, and a limiting upper bound magnitude, M_{max} have been employed. Typically, the choice of M_{max} in PI is highly uncertain because of low seismic activity, lack of fault length or fault area, and seismic catalogues being much shorter than the recurrence time of big earthquakes. In such scenarios, the statistical procedure proposed by Kijko (2004) can be used if sufficient data are available in the catalogue. The maximum magnitude can be obtained by considering an increment to the largest observed magnitude (Aldama-Bustos *et al.* 2009; Menon *et al.* 2010; Corigliano *et al.*

Table 2. *Key attributes of preselected GMPEs.*

GMPEs	No. of records	No. of earthquakes	No. of stations	Recommended M_w	Recommended R (km)	Recommended V_{S30} m/s
NDMA10	Finite fault stochastic model			4–8	1–300	1500
PEA2011	Hybrid empirical method			5–8	0–1000	$\geq$ 2000
ASB14	1041	221	322	4–7.6	0–200	150–1200
BSSA14	2100	600	–	3–8.5	0–400	150–1500
G16	5026	48	–	4–8.5	0–1000	450–2800

2012). In the present study, two values of maximum magnitudes have been considered: the maximum historical magnitude ever recorded in the region and the previous value increased by 0.5 units. The maximum magnitude adopted in this study is in line with the NDMA (2010) and Anbazhagan *et al.* (2015a) record for the Southern Craton.

5.2 *Ground-motion prediction model*

After the seismic source is characterized, GMPEs or attenuation relations are used to evaluate the ground-motion intensity measure at the required site due to the identified seismogenic sources. The GMPE is a closed-form equation linking ground motion intensity measures (IMs) (e.g., PGA, peak ground velocity (PGV) and elastic pseudo-spectral accelerations (PSAs) at various structural periods), to different predictor variables such as earthquake source, path of wave propagation, local site and fault mechanism (Douglas 2003). The southern part of PI is a region of relatively low seismicity and sparse digital strong-motion networks. The strong-motion records are almost inexistent, except for M_w 5.7 1997 Jabalpur earthquake and M_w 5.7 2001 Bhuj aftershock in the PI. There is no GMPE available for PI based on the recorded data. In view of this fact we took recourse from worldwide accepted and well-known GMPEs. Hundreds of GMPEs are available in the literature due to which a seismic hazard analyst is faced with ambiguity in deciding on the GMPEs to be used for a given project. The decision of selecting appropriate GMPEs is a very important step in hazard analysis due to their major influence on the hazard results. Therefore, the GMPEs developed for other regions with similar seismotectonic features have been examined. The preselection of GMPE is carried out by first utilizing the exclusion criteria proposed by Bommer *et al.* (2010). The pre-selected models are:

(i) National Disaster Management Authority (2010), (abbreviated as 'NDMA2010'),
(ii) Pezeshk *et al.* (2011), 'PEA2011',
(iii) Akkar *et al.* (2014), 'ASB2014',
(iv) Boore *et al.* (2014), 'BSSA2014', and
(v) Graizer (2016), 'G16'.

Table 2 sums-up important attributes of the preselected GMPEs including the number of earthquakes, recording stations and records, recommended magnitude, distance and site condition.

The control region of the present study site consists of Koyna–Waran and Killari region which are the most active regions of peninsular India. Sharma *et al.* (2007) studied attenuation of P, S, and coda waves in Koyna region, and concluded that attenuation characteristics of the Koyna region are close to active regions of the world. The stress drop considered by various researchers for active tectonic environments such as Western US is in the range of 80–135 bar (Campbell 2003; Atkinson and Silva 2000; Shahjouei and Pezeshk 2016), which is close to stress drop during Killari earthquake (45–100 bar, Seeber *et al.* 1996). Hence, considering these facts, both active and stable continental region GMPEs have been employed.

5.2.1 *GMPE comparison with strong-motion data from PI*

Attenuation of ground-motion with distance predicted by the preselected five GMPEs is compared with the strong-motion records of two earthquakes from PI. Six strong-motion records, given in table 3, from the Jabalpur (1997) earthquake and the Bhuj (2001) aftershock, both of magnitude M_w 5.7 (Singh *et al.* 2003), are used for the comparison (refer figure 8). The preselected GMPEs use different source-to-site distance definitions, and hence to facilitate a direct comparison and to use them within the logic tree framework, the distances are converted into Joyner–Boore (R_{jb}) distance

Table 3. *Strong-motion records used for comparison with selected GMPEs (after Singh et al. 2003).*

Station	R (km)	a_{max} (g) N	E	z
M_w 5.7 2001 Bhuj aftershock				
BHUJ	101	0.0075	0.0079	0.0042
DGA	249	0.0017	0.0013	0.0011
BOM	576	0.0003	0.0002	0.0002
M_w 5.7 1997 Jabalpur earthquake				
BLSP	237	0.0125	0.0116	0.0042
BHPL	271	0.006	0.0086	0.0048
BOKR	600	0.0007	0.0009	0.0004

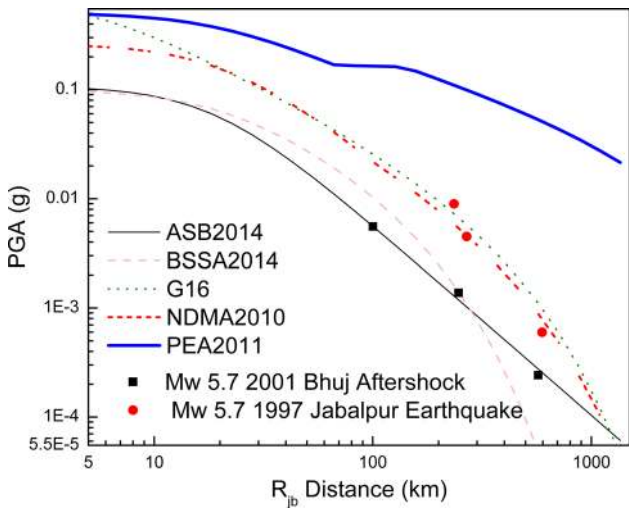

Figure 8. Comparison between preselected GMPEs and recorded PGA for Jabalpur earthquake and Bhuj aftershock (M_w 5.7).

using the algorithm based on the simulated data and gamma distribution models (Scherbaum *et al.* 2004). The GMPE-PEA2011 predicts unreasonably high PGA values (see figure 8), hence the same is discarded. The predicted values by NDMA2010 and G16 tend to be upper bounds compared to ASB2014 and BSSA2014. However, the former match the data of Jabalpur (1997) earthquake rather well. The predictions by the other two models, ASB2014 and BSSA2014, match well with the Bhuj (2001) aftershock record.

The selected four GMPEs can be compared on common sets of axes in terms of their spectral shapes, distance-scaling and magnitude-scaling, called as trellis charts, similar in format to those used in the global earthquake model (GEM) project (Stewart *et al.* 2015). These charts are helpful to display multidimensional information such as magnitude, source to site distance and structural period along with the predicted ground-motions in various ways to provide perceptivity into the selected GMPEs (Stewart *et al.* 2015). The main objective of using these charts is to identify deviations related to nonphysical behaviour and to assist in choosing the appropriate models to address the epistemic uncertainty. The trellis charts are prepared for rock site condition (i.e., $V_{s30} = 800$ m/s) for all the four GMPEs.

Figure 9 depicts PSA trellis chart for $M_w = 5$, 6 and 6.4 and $R_{jb} = 10$, 35 and 100 km using the selected GMPEs. The variability between attenuation models is much greater at short period for all magnitude and distance combinations. The same is also observed for large magnitude at short distance, which is obvious for the reason that available strong-motion data from large magnitude earthquakes at short distance is generally less. Different GMPEs have maximum spectral acceleration at different time periods because different functional forms and datasets are used by different developers. The NDMA2010 and G16 models predict consistently high values of PSAs for all magnitude and distance combinations as compared to ASB2014 and BSSA2014, which include relatively large databases.

Figure 10 shows attenuation of selected GMPEs against distance for PSA at three oscillator periods $T = 0$ (PGA), 0.3 and 1.0 s and $M_w = 5$, 6 and 6.4. All the models exhibit magnitude dependent attenuation. The effect of the inelastic attenuation can be seen from curvature in the attenuation trends. The BSSA2014, NDMA2010 and G16 models exhibit inelastic attenuation from 10 to 100 km, whereas ASB2014 does not exhibit this property. These observed inelastic attenuations are clearly apparent for PGA and 0.3 s PSA, but at 1.0 s PSA it is not apparent.

Figure 11 depicts magnitude scaling of selected GMPEs for $R_{jb} = 10$, 35 and 100 km and oscillator periods $T = 0$, 0.3 and 1.0 s. The models NDMA2010 and ASB2014 suffers from magnitude saturation (i.e., linear scaling of PSA with M_w over considered range) because of which they can give unreasonably high or low ground-motions at the boundaries of interested magnitude and distance combinations (Stewart *et al.* 2015). Magnitude saturation effects are well established by models BSSA2014 and G16. These observations coming from the trellis charts are used in assigning the weights to the GMPEs in the logic tree framework.

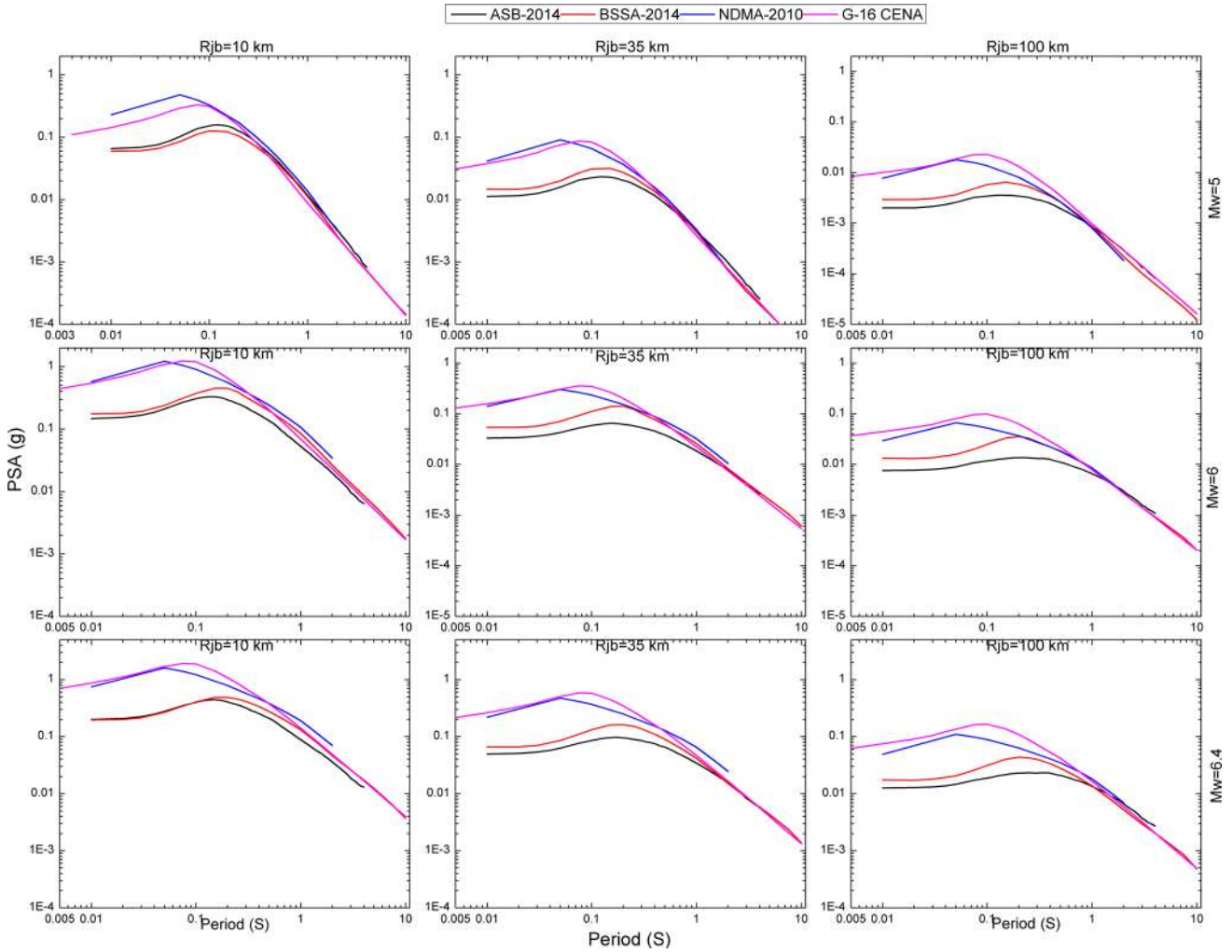

Figure 9. Trellis charts showing predicted PSAs for selected GMPEs for $M_w = 5$, 6 and 6.4; $R_{jb} = 10$, 35 and 100 km.

6. Hazard computations

The classical Cornell–McGuire (Cornell 1968; McGuire 2004) approach is employed in hazard computations. According to Baker and Gupta (2016), the annual frequency (λ) that some ground-motion intensity measure (IM) (for e.g., PGA, PSA) exceeds a selected ground-motion level x at a site is computed as follows:

$$\lambda(IM > x) = \sum_{i=1}^{n_{\text{source}}} \lambda(M_i > m_{\min}) \times \int_{m_{\min}}^{m_{\max}} \int_{0}^{r_{\max}} P(IM > x|m, r) \times f_{Mi}(m) f_{Ri}(r)\, dm\, dr \quad (1)$$

where n_{source} is the number of earthquake sources considered, $m_{\min}$ is the minimum magnitude of interest, and for source i, the magnitude and distance distribution is indicated by M_i, R_i, respectively, $f_{Mi}(m)$ and $f_{Ri}(r)$ are the probability density functions (PDFs) for magnitude and distance of an earthquake on source i, respectively and $\lambda(M_i > m_{\min})$ is the annual seismic activity rate above the threshold magnitude $m_{\min}$ on source i. The terms $\lambda(M_i > m_{\min})$, $f_{Mi}(m)$ and $f_{Ri}(r)$ constitute the seismic source characterization (SSC) part of the calculation. The term $P(IM > x|m, r)$ is the GM characterization part of hazard calculation; it is the conditional probability that an earthquake of magnitude m at distance r from the site produces a ground motion intensity measure $IM > x$. The above-described PSHA methodology is implemented in the code CRISIS 2014 (Ordaz *et al.* 2011), which is used for hazard computations in the current study.

7. Logic tree

The quantification of uncertainty is crucial in PSHA. There are two kinds of uncertainty namely,

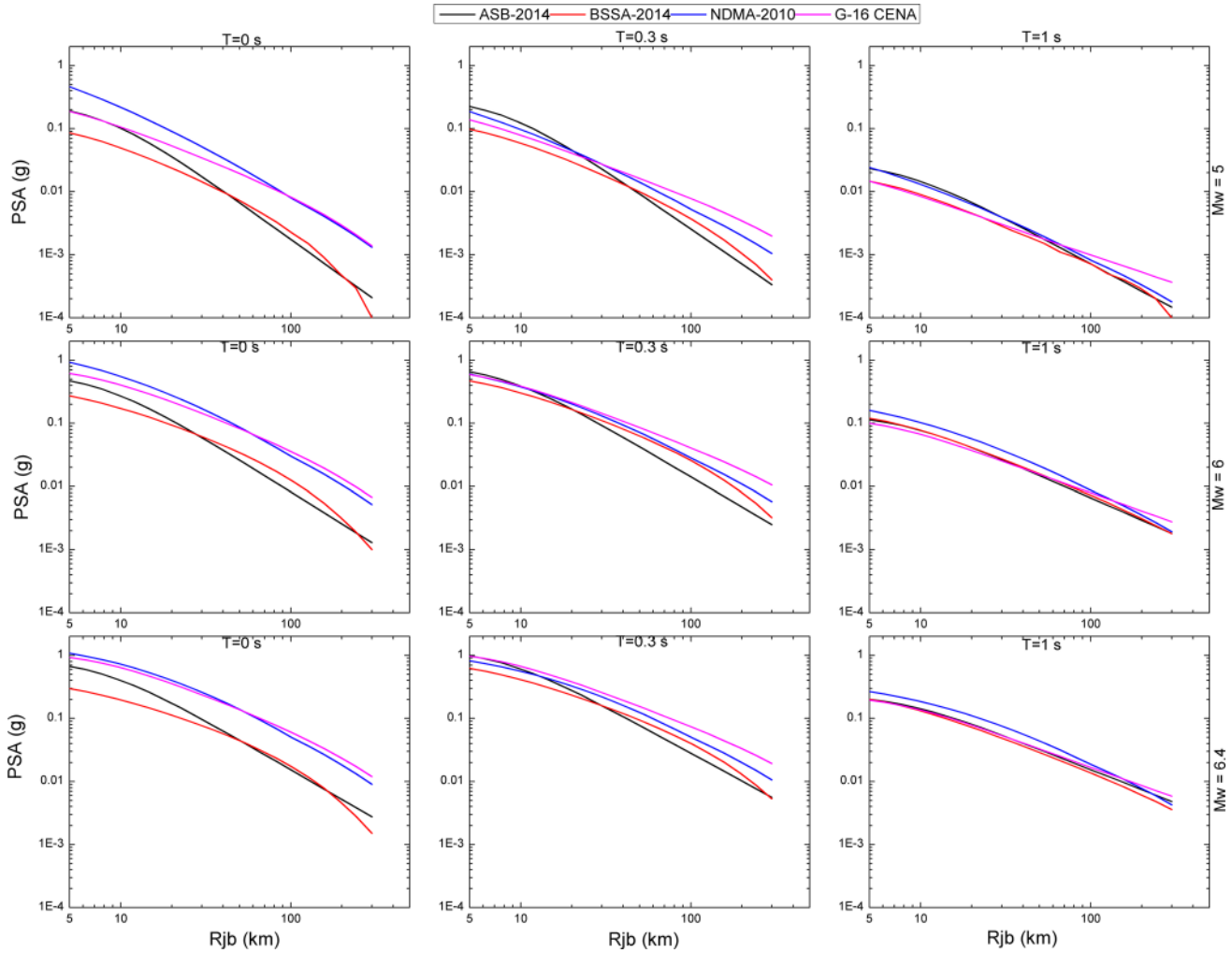

Figure 10. Trellis charts showing distance decay for selected GMPEs for M_w = 5 6 and 6.4; T = 0, 0.3 and 1 s.

epistemic uncertainty and aleatory uncertainty, the latter also called random uncertainty. Aleatory uncertainty is natural randomness in earthquake occurrence (size, location and time) and ground-motion generation, which are addressed by PDFs that are directly integrated into hazard calculation. It is the result of simplified modelling of complex process, which cannot be reduced by additional collection of data unless including more predictive parameters. Epistemic uncertainty is scientific uncertainty in the simplified model of the earthquake process, which can be reduced by additional collection of data. It is addressed traditionally by a logic tree (Kulkarni *et al.* 1984), in which alternative models are placed on different branches and assigned the weighting factor which reflects the confidence of expert on those models. A seismic hazard is evaluated for each end branch with total weighting factor equal to product of the weights on the branches leading to the corresponding end branch. Thus, epistemic uncertainty leads to family of hazard curves with weights that sum to unity. From this family of curves, the analyst can calculate mean hazard curve (McGuire 2004).

In the present study, a logic tree with 32 branches (figure 12) has been constructed: it consists of two seismogenic zoning scenarios (SZI and SZII), two earthquake catalogue completeness analysis methods (Visual cumulative, VC and Stepp), two maximum cut-off magnitudes (M1 and M2) and four GMPEs (ASB14, BSSA14, G16 and NDMA10). The assigned weighting factors are also shown in figure 12. Equal weights are assigned to the two seismogenic zoning scenarios and maximum magnitudes because there is no reason to prefer one alternative over the other. The completeness analysis method based on CUVI has been given a slightly higher weight (0.6) over the Stepp method (0.4). After thorough observation of

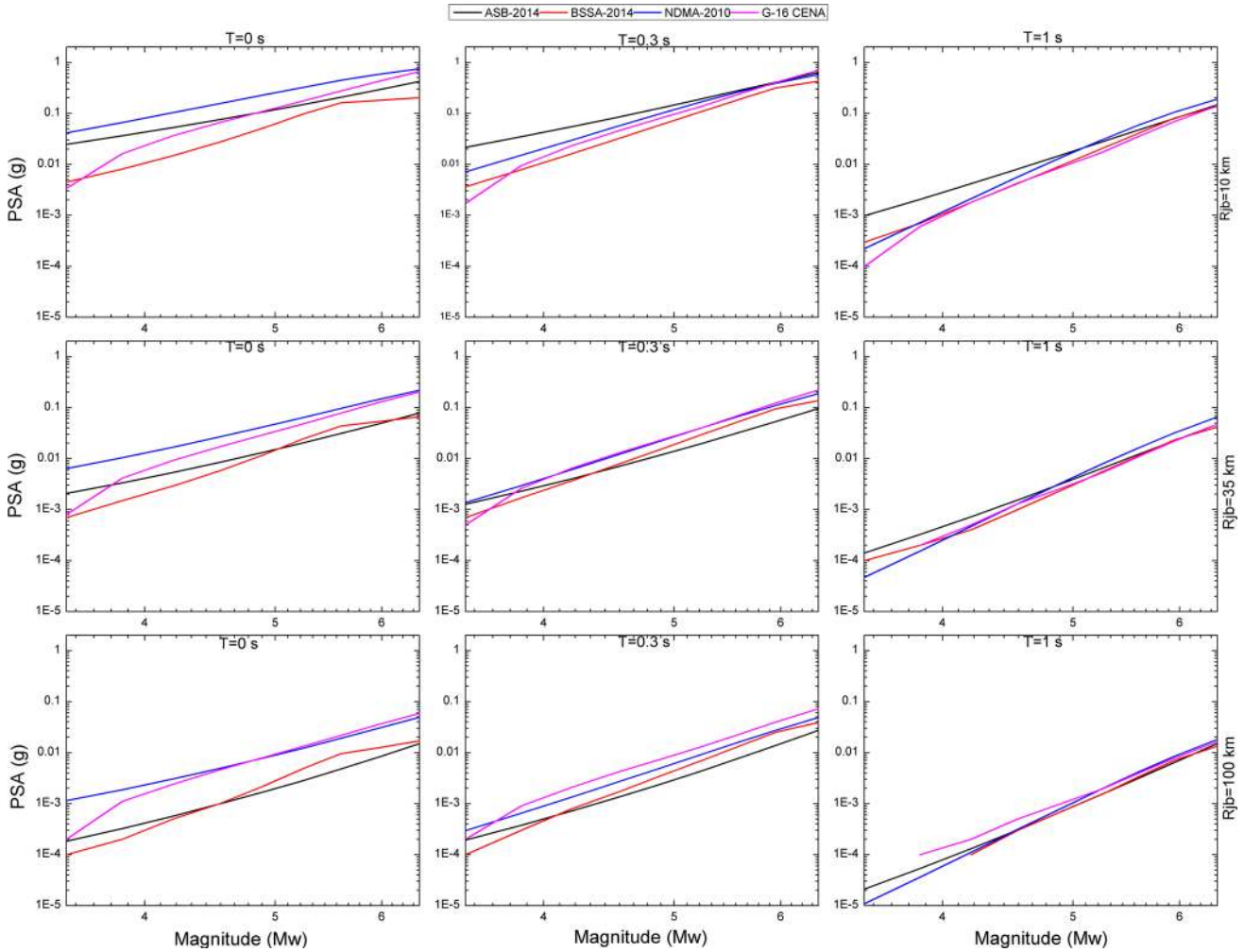

Figure 11. Trellis charts showing magnitude-scaling for selected GMPEs for $M_w = 5$, 6 and 7; $R_{jb} = 10$, 30 and 100 km.

the trellis charts and comparisons of GMPEs with strong-motion records (see section 5.2.1), the models BSSA14 and G16 are assigned a weight of 0.3 each, and a weight of 0.2 each is assigned to models NDMA10 and ASB14. The sum of the probabilities of all branches connected to a terminal node must be one (1.0).

8. PSHA results and discussion

8.1 *Seismic hazard curves*

A key outcome of PSHA is the seismic hazard curve, which is the relationship between the probability of exceedance (PE) and intensity measures (IM) such as PGA and PSAs within a specified time interval. Figure 13 shows the mean hazard curves of PGA and PSAs at $T = 0.05$, 0.1, 0.5, 1.0 s obtained at the archaeological site of Gol Gumbaz in Vijayapura.

8.2 *Uniform hazard spectrum*

Uniform hazard spectrum (UHS) is PSA ordinates with the same probability of exceedance for a considered time span. The UHS is a common result of the PSHA, often used in response spectrum analysis of structures or as the target spectrum for acceleration time-history selection and scaling. The uniform hazard spectra (UHS) for 5% damping with return periods of 72, 224, 475, 975 and 2475 years at level and stiff/rock ground conditions for the horizontal component of ground motions are derived from the hazard curves (refer figure 14; table 4).

From table 4, it can be observed that PGA and PSA values for 475- and 2475-yr return periods obtained by NDMA (2010) are less in comparison to the present results. The main reason for this underestimation can be attributed to the use of a single GMPE, which is based on the finite source

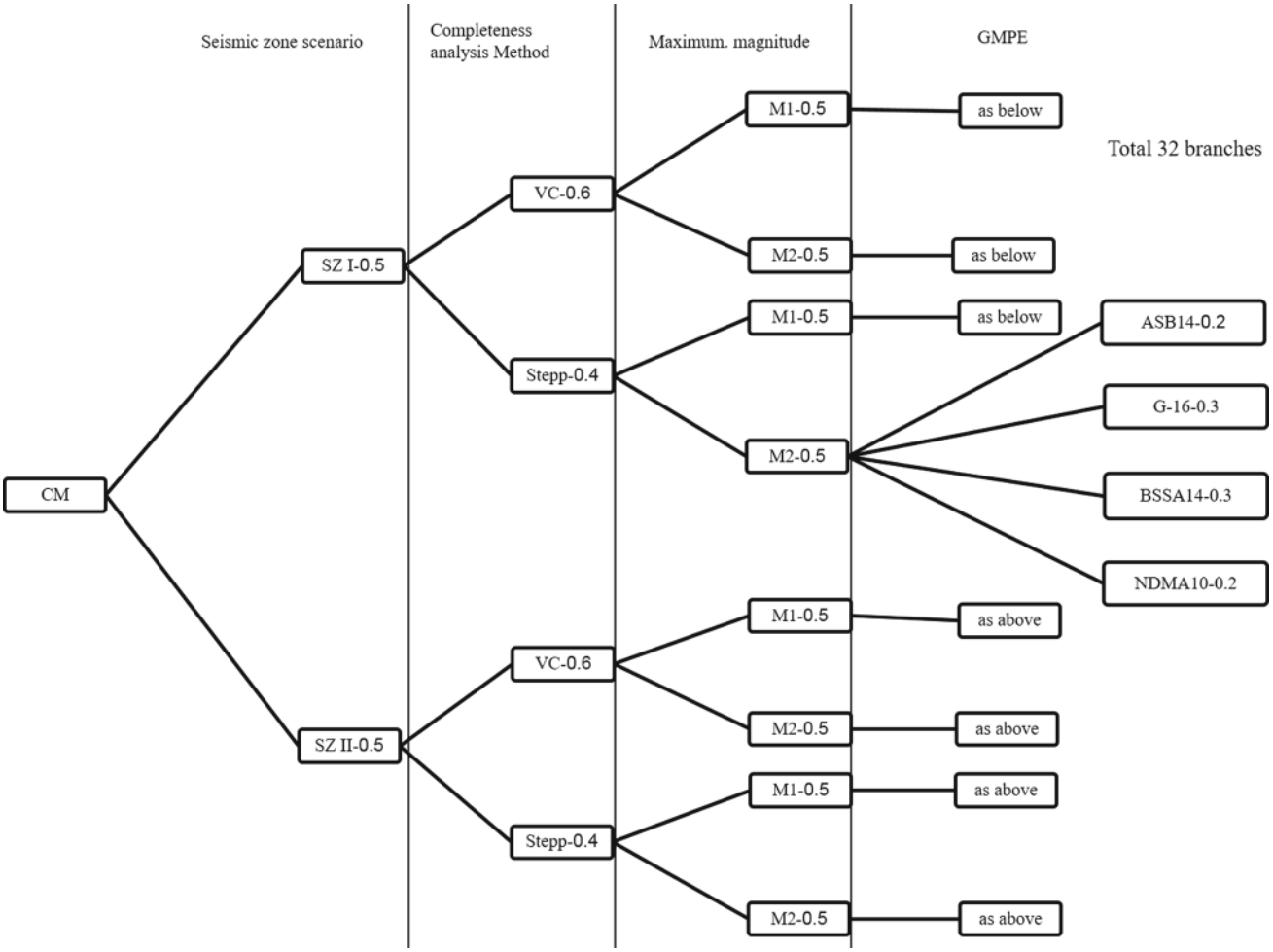

Figure 12. Parameters and weighting factors adopted in the logic tree for the horizontal ground-motion component.

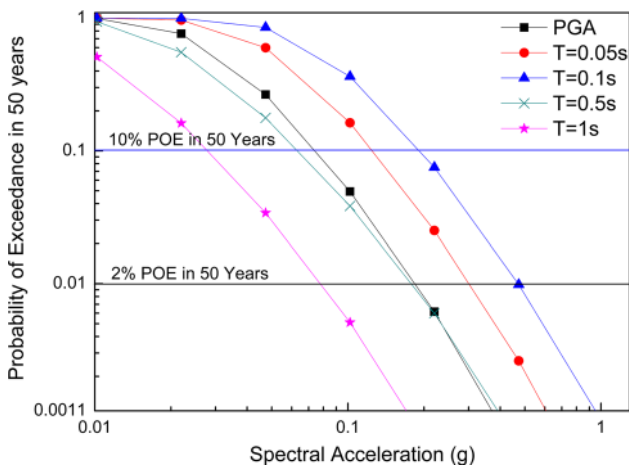

Figure 13. Seismic hazard curves for Gol Gumbaz site for different intensity measure levels.

attenuation model. The isoseismal map of Killari during 1993 $M_w = 6.4$ earthquake (refer figure 2) shows that the present site had experienced an intensity of VI on the MMI scale. According to the correlation of Trifunac and Brady (1975), the equivalent PGA for VI intensity is 0.067 g, which is in close agreement with the PGA for 475-yr RP obtained in this study. Table 5 gives the PGAs at the site calculated from different GMPEs due to Killari 1993 $M_w = 6.4$, and maximum earthquake considered (M_{max}) in the study region ($M_w = 6.9$). Table 5 also compares equivalent PGA of Killari 1993 earthquake with PGAs obtained from GMPEs.

The 475-yr RP hazard level is considered as representative of moderate events that are reasonably likely to affect the structure in its design life, which is often designated as the design basis earthquake (DBE). The 2475-yr RP hazard level represents the most severe earthquake effects considered for important structures, which is often designated as the maximum considered earthquake (MCE). Vijayapura lies in Zone III of Indian seismic code (IS: 1893 Part 1 2002) where the expected PGA for DBE and MCE, are 0.08 and 0.16 g, respectively.

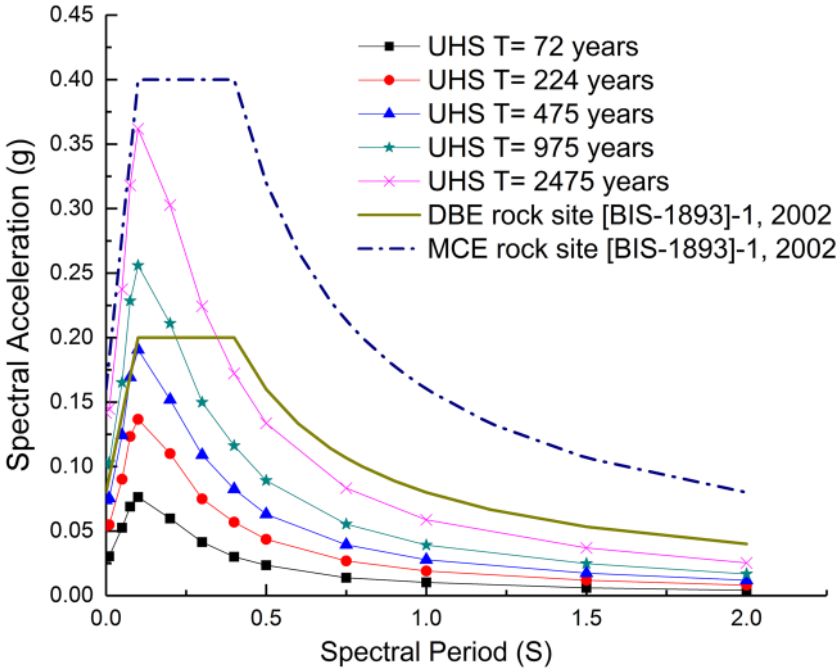

Figure 14. Comparison of the median horizontal UHS for different return periods and DBE and MCE elastic response spectra as per BIS 1893 (2002).

Table 4. *Comparison of PSAs (g) of the present study with NDMA and IS: 1893 for different return periods.*

	Present study				NDMA (2010)				IS: 1893 Part 1 (2002)			
RP (year)	$T = 0$ PGA	0.2 PSA	0.5 PSA	1 PSA	$T = 0$ PGA	0.2 PSA	0.5 PSA	1 PSA	$T = 0$ PGA	0.2 PSA	0.5 PSA	1 PSA
72	0.029	0.060	0.024	0.010	–	–	–	–				
224	0.054	0.110	0.044	0.019	–	–	–	–				
475	0.074	0.152	0.063	0.028	0.014	0.0175	0.0087	0.0042	0.08	0.2	0.16	0.08
975	0.101	0.211	0.089	0.039	–	–	–	–				
2475	0.142	0.303	0.134	0.059	0.0267	0.0333	0.0173	0.0088	0.16	0.4	0.32	0.16

Table 5. *PGAs (g) at site calculated from different GMPEs due to Killari 1993* $M_w = 6.4$ *and* $M_{max} = 6.9$ *earthquake.*

R = 160 km	NDMA2010	G16	ASB2014	BSSA2014	Isoseismal
$M_w = 6.4$	0.0267	0.0332	0.0075	0.0078	0.067
$M_w = 6.9$	0.0464	0.0589	0.014445	0.0115	–

The DBE and MCE of IS: 1893 Part 1 2002 can be associated with 475- and 2475-yr RPs respectively, though the current code definition is not probabilistic in nature. Figure 14 and table 4 also compare the UHS for 475- and 2475-year RPs at the site with the elastic design code spectra for DBE and MCE, respectively. It is seen that the PGA values compare well with the present results. However, at longer structural periods, IS code recommends higher spectral accelerations. The present results are in close agreement with some of the previous PSHA studies carried out for different regions of PI (e.g., Jaiswal and Sinha 2007 for PI; Menon *et al.* 2010 for Tamil Nadu; Corigliano *et al.* 2012 for Kancheepuram in southern India).

8.3 *Disaggregation*

The integrative process of PSHA is incapable of directly providing the parameters characterizing an earthquake (e.g., acceleration time-histories) that are representative of the computed hazard.

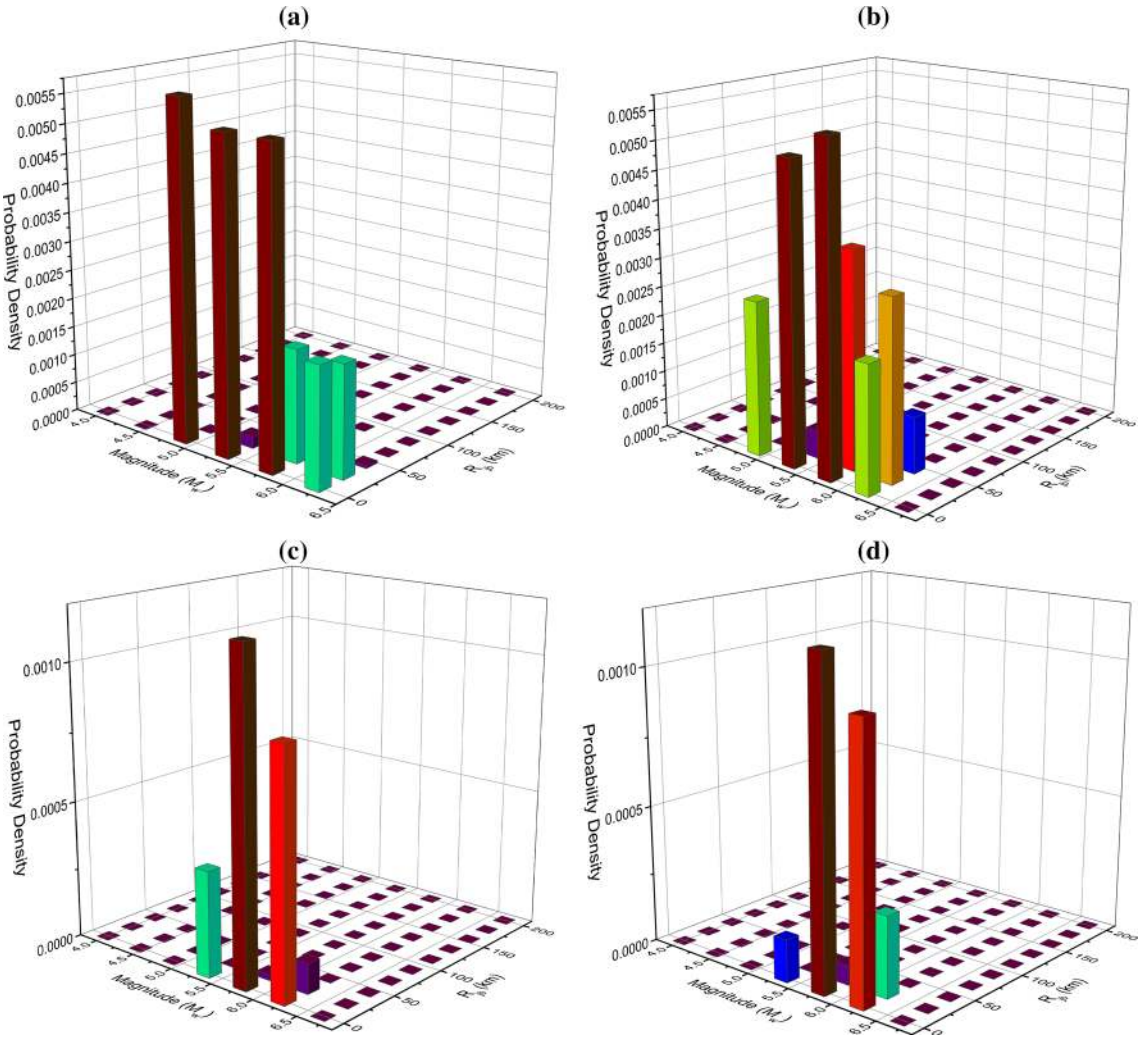

Figure 15. Disaggregation of hazard. For 475-yr RP: **(a)** PGA, **(b)** PSA at $T = 0.5$ s; for 2475-yr RP: **(c)** PGA, **(d)** PSA at $T = 0.5$ s.

This drawback is described by McGuire (1995) as the loss of design earthquake concept, which is addressed by the disaggregation process. The disaggregation analysis is a crucial step in defining driving scenarios (magnitude and source to site distance pairs) as outlined in Bazzurro and Cornell (1999). Disaggregation results depend on intensity measurement and hazard level considered, i.e., the ordinates of UHS at different oscillation periods will produce different disaggregation results. Figure 15 shows the disaggregation results of the seismic hazard for 475- and 2475-yr RPs for PGA and PSA at 0.5 s. For a 475-yr RP, small to moderate magnitude earthquakes (M_w = 4.75−5.25) occurring at short distances (R_{jb} = 5−50 km) will contribute to the hazard in terms of PGA and PSA at 0.5 s (figure 15) at the archaeological site of Gol Gumbaz, Vijayapura. For a 2475-yr RP, slightly higher magnitude earthquakes (M_w = 5.75−6.25) at short distances (R_{jb} = 5−50 km) will contribute to the hazard at the site. Therefore, the controlling scenario earthquake for the Gol Gumbaz site can be taken as M_w = 4.8−6.3 occurring at distances, R_{jb} = 5−50 km.

9. Deterministic seismic hazard analysis

Deterministic seismic hazard analysis (DSHA) is a special case of PSHA in which a few controlling earthquake scenarios (combination of magnitude and source-to-site distance) are considered. In the present study, three scenario earthquakes are considered based on the disaggregation results and earthquake catalogue: an earthquake representative of low seismicity with M_w = 4.8 at distance of 10 km; an earthquake representative of moderate seismicity with M_w = 6.3 at a distance of

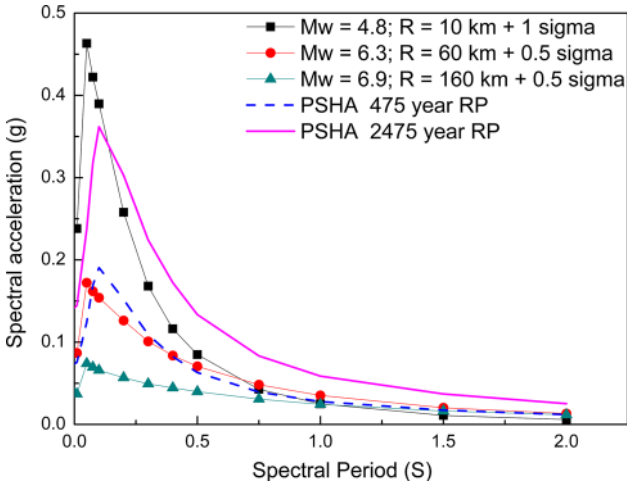

Figure 16. Comparison of the horizontal acceleration spectra (5% damping) selected based on deterministic approach with UHS of 475 and 2475 years RP.

60 km and maximum earthquake considered in the controlling area of study region, i.e., M_w = 6.9 at 160 km (i.e., the epicenter of 1993 Killari earthquake from the site). Figure 16 shows a comparison between horizontal acceleration spectra (5% damping) calculated based on the deterministic approach and horizontal UHS of the 475 and 2475 yrs RP. The GMPEs and their weights utilized in the PSHA have been used to calculate the horizontal acceleration spectra (5% damping). The effect of aleatory variability in the ground-motion prediction, normally presented as a fraction of ε of the standard deviation of the GMPE, may play an important role in comparing the results of PSHA and DSHA (Sabetta 2013). There are no specific guidelines given in the literature about the fraction of sigma to be used in the DSHA to account for the aleatory variability in the ground-motion prediction (Bommer and Abrahamson 2006; Sabetta 2013). Since small magnitude earthquakes are more likely to occur in the study region, we have used 1 sigma (i.e., ε = 1 corresponds to 16% chance of exceeding the ground-motion at the site if the selected scenario earthquake occurs) for the earthquake scenario of M_w = 4.8 at 10 km distance. For the remaining two scenarios, we have considered 0.5 sigma. The basic difference between the DSHA and PSHA is that the former considers just one (or sometimes a few) magnitude-distance-epsilon (M-D-ε) scenario, whereas the PSHA calculates the rate at which different levels of ground-motion are exceeded at the site by considering the effects of all possible combinations of M, D and ε (Bommer and Abrahamson 2006).

10. Spectrum-compatible natural ground-motions

The performance-based design philosophy requires earthquake time histories as input for linear and nonlinear response history analysis of any engineering system subjected to earthquake excitation. The response history analysis (RHA) predicts more efficiently the hierarchy of failure mechanisms, the energy absorption, force redistribution phenomena that result from gradual plastic hinge formation in a structure and contact issues (Katsanos *et al.* 2010; Sextos 2014). It is also used in the case of significant material nonlinearity. Earthquake time histories typically selected and scaled to be consistent with the UHS obtained from the PSHA, over the desired period range. Seismic safety assessment of existing structures and seismic design of new structures usually require at least seven to eleven acceleration time-histories, as prescribed by some seismic codes (e.g., Eurocode 8; FEMA 2012). The results of disaggregation analysis for the Gol Gumbaz site has provided controlling scenario earthquakes having magnitude and distance ranges as M_w = 4.8−6.3 and R_{jb} = 10−60 km, respectively. These controlling scenario earthquakes along with geological characteristics of the accelerometric station (i.e., Vs_{30} = 760−1500 m/s) are used in preselecting 15 time-history records from the Pacific Earthquake Engineering Research Center (PEER) Next Generation Attenuation (NGA) West-2 Ground Motion database (http://ngawest2.berkeley.edu/). Six compatible time-history records from NGA East Ground Motion Database (http://ngawest2.berkeley.edu/) have been preselected. Since NGA East has a limited number of earthquake ground motions from the seismic activity, restrictions on restrictive on Vs_{30} and R_{jb} were eased (Bommer and Acevedo 2004; Haselton *et al.* 2017). A further refinement is performed by additional criteria as discussed in Zimmaro (2015) to constrain the choice of the suite of ground-motions to 11.

(i) Removal of pulse-like motions: The observation of pulse-like motions due to near-fault rupture is highly unlikely in the study area; hence, these were removed from the preselected ground-motions list.
(ii) No multiple inputs from same events: Only a single record is selected from a particular earthquake event.

Table 6. *Selected horizontal ground motion components.*

Earthquake name	Station	Year	M	Mechanism	R_{jb} (km)	R_{rup} (km)	Vs30 (m/s)	MSE	SF	PGA	Tp
Coyote Lake	Gilroy Array #1	1979	5.74	Strike slip	10.21	10.67	1428	0.06	0.42	0.09	0.1
Morgan Hill	Gilroy Array #1	1984	6.19	Strike slip	14.9	14.91	1428	0.04	0.61	0.067	0.08
Chi-Chi_Taiwan-04	CHY102	1999	6.2	Strike slip	39.3	39.32	804	0.07	0.82	0.06	0.1
Umbria-03_Italy	Gubbio	1984	5.6	Normal	14.67	15.72	922	0.12	0.70	0.05	0.18
40204628	Mount Umunhum	2007	5.45	Strike slip	30.45	30.75	760	0.11	1.68	0.02	0.12
14383980	Chilao Flat Rngr Sta	2008	5.39	Reverse oblique	46.9	49.59	927	0.07	3.66	0.02	0.12
14095628	Cattani Ranch	2004	5.03	Strike slip	19.91	20.61	895	0.11	2.08	0.03	0.1
FtPayne*	Sewanee	2003	4.62	–	84.28	85.04	720	0.54	17.1	0.01	0.08
RiviereDuLoup*	HQ.CHAR	2005	4.65	–	39.44	41.75	1026	0.45	3.42	0.03	0.14
ValDesBois*	Pembroke_ON	2010	5.1	–	136.9	138.3	591	0.33	4.96	0.02	0.04
Mineral*	SE.NANPP	2011	5.74	–	18.53	20.44	553.5	0.09	0.24	0.10	0.08

*NGA: East ground motions.

(iii) Lowest usable frequencies (longest usable period): Wang *et al.* (2015) recommended that "selected records should possess lowest usable frequencies equal to or lower than the lowest frequency of interest". In the present study, ground motions with a lowest usable frequency equal or lower than of 0.4 Hz have been chosen.

(iv) No outlier motions: The mean spectrum of suite of acceleration time-histories that match well with the target spectrum may include ground-motions whose individual spectra fall far above or below the mean at some periods. Such outlier motions must be removed because they significantly affect the nonlinear response (Kramer *et al.* 2012).

(v) Time domain linear scaling: There will be a significant effect of scaling on the selected ground motion. Uniform time-domain linear scaling is adopted in order to reduce the scaling induced modifications in the selected ground-motions. In the present study, the scaling factor (SF) is set in the range of 0.2–4.0 for NGA West-2 and in the range of 0.2–18, for NGA East.

(vi) Spectral matching period range: The National Institute of Standards and Technology (NIST) published a report (NIST 2011) on selecting and scaling earthquake ground motions for performing response history analyses, which recommends the use of a period range or interval for scaling ground motions consistent with the UHS. However, no period range is given for masonry structures, hence in the present study, we used the period range (T) between 0.05 and 1 s since most structural periods of brittle masonry structures should be expected to fall in this range.

(vii) Mean squared error (MSE): It measures quantitatively how well the selected accelerograms matches with the chosen target spectrum over the selected period range. The MSE is computed using equation (2) over a user-defined period range of interest.

$$\mathrm{MSE} = \frac{\sum_i w(T_i)\{\ln[Sa_{\mathrm{target}}(T_i)] - \ln[SF \cdot Sa_{\mathrm{record}}(T_i)]\}^2}{\sum_i w(T_i)} \tag{2}$$

where SF is a linear scale factor, used to apply for the whole response spectrum of the record, T_i is the ith period and $w(T_i)$ is a weight function

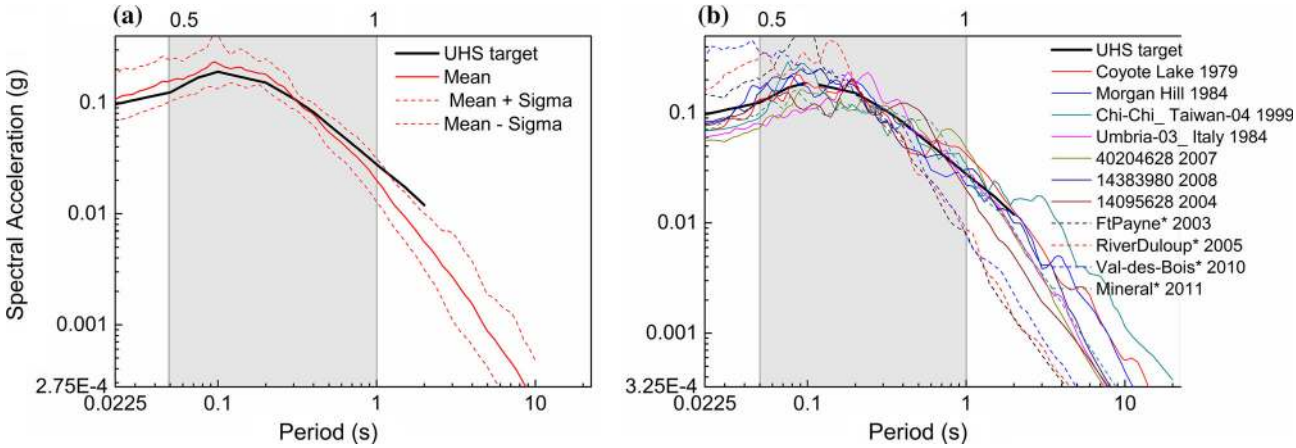

Figure 17. **(a)** The target spectrum for 475-yr RP and the mean and standard deviation response spectra of the suite and **(b)** elastic response spectra of the 11 selected and scaled accelerograms along with the target spectrum.

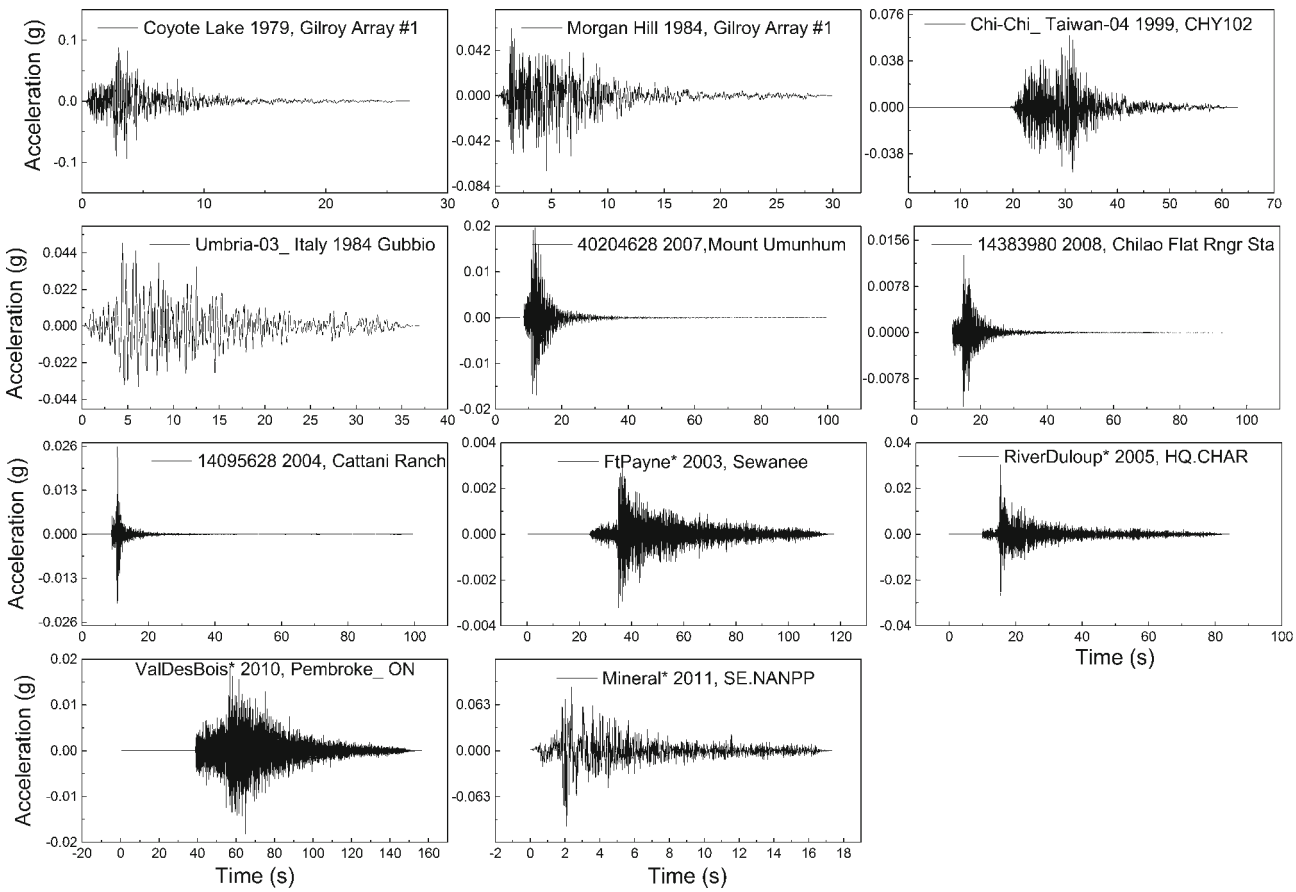

Figure 18. Selected 11 unscaled natural accelerograms corresponding to the UHS of 475-yr RP.

used to allot relative weight to different portion of the interested period range. The trivial case of $w(T_i) = 1$ is used to assign the weight for all the period of interest, i.e., from 0.05 to 1 s. The MSE provides a measure of the misfits between the spectral acceleration of the selected record and of the target spectrum, calculated using logarithms of spectral period and spectral acceleration. The actually recorded acceleration time-histories, selected to match the target spectrum of the 475-yr RP, are listed in table 6, with the MSE, SF, PGA and predominant period (T_p). The average values of MSE and SF are 0.182 and 3.46, respectively.

Figure 17(a) shows the UHS (i.e., target spectrum) for the 475-yr RP obtained from the PSHA and the mean and mean+1standard deviation (sd)

response spectra of the suite for structural damping ratio 5%. The elastic response spectra of the 11 natural accelerograms corresponding to the 475-yr RP along with the target UHS are shown in figure 17(b). The corresponding unscaled 11 natural accelerograms are shown in figure 18.

11. Conclusions

A comprehensive PSHA has been carried out for the archaeological site of Gol Gumbaz in Vijayapura, south India in order to obtain hazard-consistent natural accelerograms. Significant improvements in the PSHA have been made by adopting updated and homogeneous earthquake catalogue of the study area, new seismogenic source models and recently developed state of the art GMPE models. The quantitative enhancement of the historical earthquake information should be given a top priority in the future to have higher quality predictive computations in the future. The GMPE models are selected by comparing with a few recorded ground motions available for the PI and from the observations obtained from the trellis plots. These plots are used to assign the appropriate weights to the branches of the logic tree. The processing of all the above data with the CRISIS2014 program using the logic tree approach has led to a set of different outputs, representative of the seismic hazard at the site.

Results of the PSHA consist of horizontal hazard curves and UHS at the site for reference return periods of 72, 224, 475 and 2475 years on the rock/stiff and level ground condition. The horizontal PGA values obtained from the mean hazard curves of the logic tree at the site with 10% and 2% probabilities of exceedance in 50 years are 0.074 and 0.142 g, respectively. The spectral ordinates of the present study are comparable with the Indian code defined spectral ordinates (DBE and MCE) at short periods (0–0.125 s), whereas at long periods the code specifies higher values. The distance between source and site plays an important role, since much more active but remote area sources such as Koyna, Killari region do not impact the hazard. Based on the disaggregation of PSHA results for PGA and PSA at $T=0.5$ s, it is seen that the controlling scenario earthquakes for the study area are in the range of $M_w = 4.8-6.3$ and $R_{jb} = 10-60$ km. Computations related to the evaluation of spectrum-compatible natural ground-motions recorded on rock (i.e., $V_{s30} = 760-1500$ m/s) sites have been conducted for 10% probability of exceedance which corresponds to the UHS of 475-yr return period. Based on the pre-set selection criteria, a suite of 11 recorded acceleration time-histories are selected to match the target spectrum corresponding to the UHS of 475-yr RP, details of which are provided in the paper. These acceleration time-histories play a crucial role in the seismic risk estimation and design of seismic retrofit or strengthening measures for heritage structures.

Though the study is focussed on the application of internationally accepted approaches for seismic hazard assessment, the paper provides a methodology to arrive at different forms of seismic input required for structural assessment, that could be adopted for a region characterised by low to moderate seismicity, but with past seismic activity not too far away, and with almost no instrumental record of earthquakes.

Acknowledgements

The authors would like to thank Dr Vladimir Graizer for providing the MATLAB code for G-16 GMPE and for productive discussions of the results and Prof. Mario Gustavo Ordaz for providing CRISIS 2014 code. The authors also thank Dr G Kalyan Kumar for his timely technical assistance.

References

Akkar S, Sandıkkaya M A and Bommer J J 2014 Empirical ground-motion models for point- and extended-source crustal earthquake scenarios in Europe and the Middle East; *Bull. Earthq. Eng.* **12(1)** 359–387.

Aldama-Bustos G, Bommer J J, Fenton C H and Stafford P J 2009 Probabilistic seismic hazard analysis for rock sites in the cities of Abu Dhabi, Dubai and Ra's Al Khaymah, United Arab Emirates; *Georisk* **3(1)** 1–29.

Allen T I, Adams J and Halchuk S 2015 The seismic hazard model for Canada?: Past, present and future; *Proceedings of the Tenth Pacific Conference on Earthquake Engineering*, pp. 1–8.

Anbazhagan P, Vinod J S and Sitharam T G 2009 Probabilistic seismic hazard analysis for Bangalore; *Nat. Hazards* **48(2)** 145–166.

Anbazhagan P, Smitha C V, Kumar A and Chandran D 2013 Seismic hazard assessment of NPP site at Kalpakkam, Tamil Nadu, India; *Nucl. Eng. Des.* **259** 41–64.

Anbazhagan P, Bajaj K, Moustafa S S R and Al-Arifi N S 2015a Maximum magnitude estimation considering the regional rupture characteristics; *J. Seismol.* **19(3)** 695–719.

Anbazhagan P, Sreenivas M, Bajaj K, Moustafa S S R and Al-Arifi N S 2016 Selection of ground motion prediction equation for seismic hazard analysis of peninsular India; *J. Earthq. Eng.*, https://doi.org/10.1080/13632469.2015.1104747.

Anbazhagan P, Bajaj K, Dutta N, R Moustafa S S and Al-Arifi N S 2017 Region-specific deterministic and probabilistic seismic hazard analysis of Kanpur city; *J. Earth Syst. Sci.* **126(1)** 12.

Atkinson G M and Silva W 2000 Stochastic modeling of California ground motions; *Bull. Seismol. Soc. Am.* **90(2)** 255–274.

Baker J W and Gupta A 2016 Bayesian treatment of induced seismicity in probabilistic seismic hazard analysis; *Bull. Seismol. Soc. Am.* **106(3)** 860–870.

Bazzurro P and Cornell C A 1999 Disaggregation of seismic hazard; *Bull. Seismol. Soc. Am.* **89(2)** 501–520.

Bilham R, Bendick R and Wallace K 2003 Flexure of the Indian plate and intraplate earthquakes; *Proc. Indian Acad. Sci., Earth Planet. Sci.* **112(3)** 315–329.

BMTPC 1997 Vulnerability Atlas of India: Earthquake, Windstorm and Flood Hazard Maps and Damaged Risk to Housing, Ministry of Housing & Urban Poverty Alleviation, First Revision, Government of India.

Bommer J J and Acevedo A B 2004 The use of real earthquake accelerograms as input to dynamic analysis; *J. Earthq. Eng.* **8(1)** 43–91.

Bommer J J and Abrahamson N 2006 Why do modern probabilistic seismic hazard analyses often lead to increased hazard estimates?; *Bull. Seismol. Soc. Am.* **96(6)** 1967–1977.

Bommer J J, Douglas J, Scherbaum F, Cotton F, Bungum H and Fäh D 2010 On the selection of ground-motion prediction equations for seismic hazard analysis; *Seismol. Res. Lett.* **81(5)** 783–793.

Boore D M, Stewart J P, Seyhan E and Atkinson G M 2014 NGA-West2 equations for predicting PGA, PGV, and 5% damped PSA for shallow crustal earthquakes; *Earthq. Spectra* **30(3)** 1057–1085.

Campbell K W 2003 Prediction of strong ground motion using the hybrid empirical method and its use in the development of ground-motion (attenuation) relations in eastern north America; *Bull. Seismol. Soc. Am.* **93(3)** 1012–1033.

Chandra U 1977 Earthquakes of peninsular India – a seismotectonic study; *Bull. Seismol. Soc. Am.* **67(5)** 1387–1413.

Copley A, Mitra S, Sloan R A, Gaonkar S and Reynolds K 2014 Active faulting in apparently stable peninsular India: Rift inversion and a Holocene-age great earthquake on the Tapti Fault; *J. Geophys. Res.-Solid Earth* **119(8)** 6650–6666.

Corigliano M, Lai C G, Menon A and Ornthammarath T 2012 Seismic input at the archaeological site of Kancheepuram in southern India; *Nat. Hazards* **63(2)** 845–866.

Cornell C A 1968 Engineering seismic risk analysis; *Bull. Seismol. Soc. Am.* **58(5)** 1583–1606.

Dasgupta S, Pande P, Ganguly D, Iqbal Z, Sanyal K, Venkataraman N V, Sural B, Harendra-nath L, Mazumdar K, Sanyal S, Roy A, Das LK, Misra P S and Gupta H K 2000 Seismotectonic Atlas of India and its Environs; *Spec. Publ. Geol. Surv. India*.

Desai S S and Choudhury D 2013 Spatial variation of probabilistic seismic hazard for Mumbai and surrounding region; *Nat. Hazards* **71** 1873–1898.

Douglas J 2003 Earthquake ground motion estimation using strong-motion records: A review of equations for the estimation of peak ground acceleration and response spectral ordinates; *Earth-Sci. Rev.* **61(1–2)** 43–104.

Douglas J 2016 Ground motion prediction equations 1964–2016; http://www.gmpe.org.uk.

Federal Emergency Management Agency (FEMA) 2012 Seismic performance assessment of buildings, FEMA P-58, prepared by the Applied Technology Council for the Federal Emergency Management Agency.

Gardner J and Knopoff L 1974 Is the sequence of earthquakes in southern California, with aftershocks removed, Poissonian; *Bull. Seismol. Soc. Am.* **64(5)** 1363–1367.

Graizer V 2016 Ground-motion prediction equations for central and eastern North America; *Bull. Seismol. Soc. Am.* **106(4)** 1600–1612.

Guha S K and Basu P C 1993 Catalogue of earthquakes ($\geq$ M 3.0) in peninsular India; AERB technical document, Anushakti Nagar Bombay, India.

Gupta I D 2006 Delineation of probable seismic sources in India and neighbourhood by a comprehensive analysis of seismotectonic characteristics of the region; *Soil Dyn. Earthq. Eng.* **26(8)** 766–790.

Gupta S, Rai S S, Prakasam K S, Srinagesh D, Bansal B K, Chadha R K, Priestley K and Gaur V K 2003 The nature of the crust in southern India: Implications for Precambrian crustal evolution; *Geophys. Res. Lett.* **30(8)** 1419.

Gutenberg B and Richter C F 1944 Frequency of earthquakes in California; *Bull. Seismol. Soc. Am.* **34(4)** 185.

Haselton C B, Baker J W and Stewart J P *et al.* 2017 Response history analysis for the design of new buildings in the NEHRP provisions and ASCE/SEI 7 standard: Part I. Overview and specification of ground motions; *Earthq. Spectra* 33:032114EQS039M, https://doi.org/10.1193/032114EQS039M.

Iyenger R N, Sharma D and Siddiqui J M 1999 Earthquake history of India in medieval times; *Indian J. History Sci.* **34(3)** 181–237.

Jaiswal K and Sinha R 2007 Probabilistic seismic-hazard estimation for peninsular India; *Bull. Seismol. Soc. Am.* **97(1)** 318–330.

Jain S K 2016 Earthquake safety in India: Achievements, challenges and opportunities; *Bull. Earthq. Eng.* **14(5)** 1337–1436.

James N, Sitharam T G, Padmanabhan G and Pillai C S 2014 Seismic microzonation of a nuclear power plant site with detailed geotechnical, geophysical and site effect studies; *Nat. Hazards* **71(1)** 419–462.

Johnston A C 1996 Seismic moment assessment of earthquakes in stable continental regions – I. Instrumental seismicity; *Geophys. J. Int.* **124(2)** 381–414.

Johnston A C and Kanter L R 1990 Earthquakes in stable continental crust; *Scientific American* **262(3)** 68–75.

Katsanos E I, Sextos A G and Manolis G D 2010 Selection of earthquake ground motion records: A state-of-the-art

review from a structural engineering perspective; *Soil Dyn. Earthq. Eng.* **30(4)** 157–169.

Kayal J R 2000 Seismotectonic study of the two recent SCR earthquakes in central India; *J. Geol. Soc. India* **55(2)** 123–138.

Kijko A 2004 Estimation of the maximum earthquake magnitude, mmax, Pure and Applied Geophysics **161** 1–27.

Kolathayar S and Sitharam T G 2012 Characterization of regional seismic source zones in and around India; *Seismol. Res. Lett.* **83(1)** 77–85.

Kramer S L 1996 Geotechnical Earthquake Engineering; In: *Prentice-Hall International Series in Civil Engineering and Engineering Mechanics*, Prentice-Hall, New Jersey.

Kramer S L, Arduino P and Sideras S S 2012 Earthquake ground motion selection; The State of Washington Department of Transportation, University of Washington.

Kulkarni R B, Youngs R R and Coppersmith K J 1984 Assessment of confidence intervals for results of seismic hazard analysis; *8th World Conf. Earthq. Eng.*, pp. 263–270.

Kumar P, Yuan X, Kumar M R, Kind R, Li X and Chadha R K 2007 The rapid drift of the Indian tectonic plate; *Nature* **449(7164)** 894–897.

Mandal P, Manglik A and Singh R 1997 Intraplate stress distribution induced by topography and crustal density heterogeneities beneath the Killari, India, region; *J. Geophys. Res.* **102(B6)** 719–729.

McGuire R K 1976 EQRISK: FORTRAN computer program for seismic risk analysis.

McGuire R K 1995 Probabilistic seismic hazard analysis and design earthquakes: closing the loop; Bull. Seismol. Soc. Am. **85** 1275–1284.

McGuire R K 2004 Seismic hazard and risk analysis; Earthquake Engineering Research Institute, Berkeley, California.

McGuire R K and Arabasz W J 1990 An introduction to probabilistic seismic hazard analysis; *Geotech. Environ. Geophys.*, pp. 333–353.

Menon A, Ornthammarath T, Corigliano M and Lai C G 2010 Probabilistic seismic hazard macrozonation of Tamil Nadu in southern India; *Bull. Seismol. Soc. Am.* **100(3)** 1320–1341.

Molina S, Lindholm C D and Bungum H 2001 Probabilistic seismic hazard analysis: Zoning free versus zoning methodology; *Bollettino di Geofisica Teorica ed Applicata* **42(1–2)** 19–39.

Nath S K and Thingbaijam K K S 2011 Peak ground motion predictions in India: An appraisal for rock sites; *J. Seismol.* **15** 295–315.

Nath S K and Thingbaijam K K S 2012 Probabilistic seismic hazard assessment of India; *Seismol. Res. Lett.* **83(1)** 135–149.

NDMA 2010 Development of probabilistic seismic hazard map of India; Technical Report by National Disaster Management Authority, Government of India.

NIST 2011 Selecting and Scaling Earthquake Ground Motions for Performing Response History Analysis; Gaithersburg, Maryland.

Ordaz M, Martinelli F, Aguilar A, Arboleda J, Meleti C and D'Amico V 2011 CRISIS2014 Ver 1.2: Program for computing seismic hazard; Institute of Engineering, UNAM, Mexico.

Pezeshk S, Zandieh A and Tavakoli B 2011 Hybrid empirical ground-motion prediction equations for eastern North America using NGA models and updated seismological parameters; *Bull. Seismol. Soc. Am.* **101(4)** 1859–1870.

Rao B R and Rao P S 1984 Historical seismicity of peninsular India; *Bull. Seismol. Soc. Am.* **74(6)** 2519–2533.

Sabetta F 2013 Seismic hazard and design earthquakes for the central archaeological area of Rome; *Bull. Earthq. Eng.* **12(3)** 1307–1317.

Scandella L, Lai C G, Spallarossa D and Corigliano M 2011 Ground shaking scenarios at the town of Vicoforte, Italy; *Soil Dyn. Earthq. Eng.* **31(5–6)** 757–772.

Scherbaum F, Schmedes J and Cotton F 2004 On the conversion of source-to-site distance measures for extended earthquake source models; *Bull. Seismol. Soc. Am.* **94(3)** 1053–1069.

Senior Seismic Hazard Analysis Committee (SSHAC) and Budnitz R J 1997 Recommendations for Probabilistic Seismic Hazard Analysis: Guidance on Uncertainty and Use of Experts (Vol. 1); Washington DC.

Sextos A G 2014 Selection of ground motions for response history analysis; *Encyclopedia of Earthquake Engineering*, Springer Berlin Heidelberg, Berlin, Heidelberg, pp. 1–10.

Shahjouei A and Pezeshk S 2016 Alternative hybrid empirical ground-motion model for central and eastern North America using hybrid simulations and NGA-West2 models; *Bull. Seismol. Soc. Am.* **106(2)** 734–754.

Sharma B, Teotia S S and Kumar D 2007 Attenuation of P, S, and coda waves in Koyna region, India; *J. Seismol.* **11(3)** 327–344.

Singh S K, Bansal B K, Bhattacharya S N, Pacheco J F, Dattatrayam R S, Ordaz M, Suresh G, Kamal and Hough S E 2003 Estimation of ground motion for Bhuj (26 January 2001; Mw 7.6 and for future earthquakes in India; *Bull. Seismol. Soc. Am.* **93(1)** 353–370.

Sitharam T G, James N, Vipin K S and Ganesha Raj K 2012 A study on seismicity and seismic hazard for Karnataka state; *J. Earth Syst. Sci.* **121(2)** 475–490.

Stepp J C 1972 Analysis of the completeness of the earthquake sample in the Puget Sound area and its effect on statistical estimates of earthquake hazard; In: *Proc. Int. Conf. on Microzonation for Safer Construct: Research and Application*, Seattle, Washington, pp. 1189–1207.

Stewart J P, Douglas J, Javanbarg M, Bozorgnia Y, Abrahamson N, Boore D M, Campbell K W, Delavaud E, Erdik M and Stafford P J 2015 Selection of ground motion prediction equations for the global earthquake model; *Earthq. Spectra* **31(1)** 19–45.

Tinti S and Mulargia F 1985 An improved method for the analysis of the completeness of a seismic catalogue; *Lettere Al Nuovo Cimento Series 2* **42(1)** 21–27.

Trifunac M D and Brady A G 1975 On the correlation of seismic intensity scales with the peaks of recorded strong ground motion; *Bull. Seismol. Soc. Am.* **65(1)** 139–162.

Valdiya K S 2016 The Making of India. Social Scientist; Society of Earth Scientists Series, Springer International Publishing, Cham.

Verma M and Bansal B K 2016 Active fault research in India: Achievements and future perspective; *Geomat. Nat. Hazards and Risk* **7(1)** 65–84.

Vita-Finzi C 2004 Buckle-controlled seismogenic faulting in peninsular India; *Quat. Sci. Rev.* **23(23–24)** 2405–2412.

Wang G, Youngs R, Power M and Li Z 2015 Design ground motion library: An interactive tool for selecting earthquake ground motions; *Earthq. Spectra* **31(2)** 617–635.

Wiemer S 2001 A software package to analyse seismicity: ZMAP; *Seismol. Res. Lett.* **72(2)** 373–382.

Zimmaro P 2015 Seismic response of the farneto del principe dam in Italy using hazard-consistent and site-specific ground motions; Thesis, Università della Calabria, Italy.

Corresponding editor: P S Agram